TS-MOF: Two-Stage Multi-Objective Fine-tuning for Long-Tailed Recognition

Zhe Zhao^{1,2} **Zhiheng Gong**^{1} **Pengkun Wang**^{1,3*} **HaiBin Wen**^{2} **Cankun Guo**^{5}
Bo Xue^{2} **Xi Lin**^{2} **Zhenkun Wang**^{4} **Qingfu Zhang**^{2} **Yang Wang**^{1,3,6*}
^{1}University of Science and Technology of China ^{2}City University of Hong Kong
^{3}Suzhou Institute for Advanced Research, USTC ^{4}Southern University of Science and Technology
^{5}Nanchang University ^{6}Anhui Provincial Key Laboratory of High Performance Computing

Abstract

Long-Tailed Recognition (LTR) presents a significant challenge due to extreme class imbalance, where existing methods often struggle to balance performance across head and tail classes. Directly applying multi-objective optimization (MOO) to leverage multiple LTR strategies can be complex and unstable. To address this, we propose TS-MOF (Two-Stage Multi-Objective Fine-tuning), a novel framework that strategically decouples feature learning from classifier adaptation. After standard pre-training, TS-MOF freezes the feature backbone and focuses on an efficient multi-objective fine-tuning of specialized classifier heads. The core of TS-MOF's second stage lies in two innovations: Refined Performance Level Agreement for adaptive task weighting based on real-time per-class performance, and Robust Deterministic Projective Conflict Gradient for stable gradient conflict resolution and constructive fusion. This approach enables effective synergy between diverse LTR strategies, leading to significant and balanced performance improvements. Extensive experiments on CIFAR100-LT, ImageNet-LT, and iNaturalist 2018 demonstrate that TS-MOF achieves state-of-the-art results, particularly enhancing tail class accuracy (e.g., +3.3% on CIFAR100-LT IR=100 tail) while improving head class performance, all within a remarkably short fine-tuning period of 20 epochs. We provide the detailed code in https://github.com/DataLab-atom/TS-MOF.

1 Introduction

The ubiquitous long-tailed distribution of real-world visual data presents a formidable obstacle to training deep learning models that can generalize well across all categories [21, 3]. Models trained on such imbalanced datasets inevitably develop a bias towards data-rich head classes, leading to significantly deficient performance on data-scarce tail classes. Although numerous Long-Tailed Recognition (LTR) strategies have been proposed—spanning resampling [4, 2], loss re-weighting [19, 5], and advanced representation learning [13, 29]—they often suffer from the "seesaw dilemma": efforts to enhance tail class performance frequently come at the cost of head class accuracy, exposing an inherent trade-off that is difficult to perfectly reconcile with a single strategy.

Given the limitations of individual strategies and the tendency for different LTR methods to exhibit unique strengths across various class regions, "multi-strategy collaboration" has emerged as an attractive research direction. Recently, ideas from Multi-Objective Optimization (MOO) [26, 6] and strategy fusion [27] have begun to be introduced into the LTR domain, attempting to find more balanced solutions by jointly optimizing multiple conflicting objectives. However, directly applying multiple complex LTR strategies to end-to-end training of an entire network can lead to

[*]Corresponding author.

substantial computational overhead and tuning difficulties. It may also result in suboptimal feature representations and unstable training dynamics due to potential conflicts between strategies and interference with the feature learning process. This complexity has limited the widespread application and usability of advanced MOO concepts in the LTR field.

To address these challenges, we propose TS-MOF (Two-Stage Multi-Objective Fine-tuning), a novel LTR framework. The core idea of TS-MOF lies in strategic decoupling: first, high-quality generic feature representations are obtained through standard pre-training; subsequently, with this feature backbone frozen, the focus shifts to efficiently fine-tuning a set of classifier heads specifically designed for LTR using multi-objective optimization. This two-stage design significantly lowers the barrier to combining multiple LTR strategies with MOO, as the complex MOO process acts only on the classifier heads, which have fewer parameters, and without the risk of corrupting well-learned features. This enhances overall training robustness and methodological ease of use. Notably, this targeted multi-objective adaptation process is highly efficient; we demonstrate that it can be completed within a very short fine-tuning period (e.g., just 20 epochs) while achieving excellent performance.

The efficacy of TS-MOF hinges on its sophisticated multi-objective optimization mechanism in the second stage, driven by two core innovations that ensure effective integration and synergy of knowledge from different LTR strategies:

1. **Refined Performance Level Agreement (R-PLA) Weighting:** R-PLA is an adaptive dynamic task weighting mechanism that surpasses traditional fixed or simple heuristic weight assignments. By evaluating the instantaneous accuracy of each LTR strategy ("task") on various classes in real-time and combining this with its cosine similarity to a preset reference performance pattern (transformed by a cube root and non-negative clipping for enhanced robustness and differentiability), R-PLA intelligently identifies and amplifies signals from strategies that contribute most to improving critical class performance at the current learning stage. This ensures that optimization resources are directed towards the most effective paths within the limited fine-tuning window.

2. **Robust Deterministic Projective Conflict Gradient (RD-PCGrad):** To resolve gradient conflicts and negative transfer issues that may arise when updating parameters with multiple LTR strategies, we developed RD-PCGrad. This technique is a significant enhancement over existing conflict-avoidance gradient methods (like PCGrad). By performing deterministic iterative projections and numerically stable aggregation of task gradients (weighted by R-PLA), it forms a Pareto-improving direction. RD-PCGrad not only guarantees the reproducibility and training stability of the multi-task learning process—crucial for convergence in a short time—but more importantly, it enables the constructive fusion of heterogeneous knowledge from different LTR strategies (e.g., some focusing on class balance, others on hard-sample mining), jointly propelling the model towards a more balanced and superior performance state.

During inference, we employ the Evolving Optimal Strategy Selection (EOSS) mechanism [32] to integrate predictions from the different classifier heads. The core performance improvements and unique advantages of TS-MOF, however, primarily stem from the efficient, stable, and synergistic multi-objective fine-tuning process during training, driven by R-PLA and RD-PCGrad on the frozen feature foundation.

We validate the superior performance of the TS-MOF framework through extensive experiments on several challenging LTR benchmark datasets, including CIFAR100-LT, ImageNet-LT, and iNaturalist 2018. The experimental results demonstrate that TS-MOF not only surpasses existing state-of-the-art (SOTA) methods in overall accuracy across various benchmarks but also achieves significant breakthroughs in crucial tail-class recognition accuracy, while also improving or effectively maintaining head-class performance. For instance, on the most challenging CIFAR100-LT (IR=100) benchmark, TS-MOF achieves **56.8%** overall accuracy and **39.9%** tail accuracy, a significant improvement over the previous SOTA method LOS [27] (53.9% overall, 36.6% tail), with head accuracy also increasing from 70.3% to 79.0%—all within an efficient 20-epoch fine-tuning budget. These results fully substantiate that our strategy of two-stage decoupling combined with advanced MOO components offers a robust, user-friendly, and efficient solution for tackling complex long-tailed recognition problems. We will release our code and pre-trained models to foster further research in the community.

2 Related Work

2.1 Long-Tailed Recognition

Long-Tailed Recognition (LTR) addresses the challenge of learning from datasets where class distributions are heavily skewed, with a few head classes having abundant samples and many tail classes having very few. Initial efforts focused on **data re-sampling**, either by over-sampling tail classes [4] or under-sampling head classes [2, 9]. However, naive over-sampling can lead to overfitting on tail classes, while under-sampling discards valuable data from head classes.

Another prominent direction is **loss re-weighting**, which aims to assign higher importance to samples from tail classes during training. Techniques like Focal Loss [19] down-weight easy examples, indirectly helping with class imbalance, and have inspired further work such as Focal-SAM which combines focal-style weighting with sharpness-aware minimization [18]. More directly, methods like Class-Balanced Loss [5] re-weight the loss based on the effective number of samples per class. Label-Distribution-Aware Margin (LDAM) loss [3] enforces larger margins for minority classes, and Balanced Softmax [25] adjusts the softmax function to account for class frequencies. Other approaches modify the logits directly to achieve re-balancing, such as through Gaussian-based adjustments [15]. The theoretical underpinnings of re-weighting and logit-adjustment have also been explored to provide a unified understanding of their generalization properties in imbalanced learning [30].

Representation learning and knowledge transfer techniques seek to learn more robust and generalizable features, or transfer knowledge from head to tail classes. Methods like BBN [33] use a two-branch network to learn representations and perform cumulative learning. Other approaches focus on feature augmentation for tail classes, disentangling feature norms from directions [20], or fusing features from head to tail classes to improve representations [17]. Some research delves into the intrinsic properties of learned features, unveiling and mitigating biases by analyzing perceptual manifolds [22]. Recently, adapting large pre-trained models using visual prompt tuning has emerged as a promising direction, with methods designed to improve performance on tail classes [16, 11]. Multi-expert models, such as RIDE [29], train diverse experts specialized in different parts of the data distribution.

2.2 Two-Stage Long-Tailed Learning

Recognizing the difficulty of simultaneously learning good features and a balanced classifier on long-tailed data, two-stage approaches have gained significant traction. The seminal work by Kang et al.[13] proposed decoupling representation learning from classifier learning. In their framework, features are first learned using instance-balanced sampling, and then the classifier is re-trained or adjusted using class-balanced sampling or other techniques like logit adjustment[24]. This decoupling strategy allows the backbone network to learn general and high-quality features without being overly biased by the imbalanced data distribution during the initial stage. Subsequent works have built upon this paradigm. For example, LOS [27] explores an optimal strategy within a two-stage framework by adaptively combining multiple re-balancing strategies. Our proposed TS-MOF framework also adopts a two-stage design, but uniquely focuses the second stage on a sophisticated multi-objective fine-tuning of specialized classifier heads using novel components like R-PLA and RD-PCGrad.

2.3 Multi-Objective Optimization in Deep Learning

Multi-Objective Optimization (MOO) is concerned with simultaneously optimizing multiple, often conflicting, objectives. In deep learning, MOO has been increasingly applied to multi-task learning (MTL) and problems with inherent trade-offs. Sener and Koltun [26] framed MTL as MOO, proposing methods to find Pareto optimal solutions by optimizing a weighted sum of losses or manipulating gradients. Gradient manipulation techniques are particularly relevant. For instance, MGDA (Multiple Gradient Descent Algorithm)[7] finds a common descent direction that improves all tasks. PCGrad (Projective Conflict Gradient)[31] mitigates conflicting gradients between tasks by projecting a task's gradient onto the normal plane of another task's gradient if they conflict. Our RD-PCGrad builds upon such principles to ensure stable and deterministic conflict resolution. The goal of MOO is often to find a set of solutions on the Pareto front, where no objective can be improved without degrading at least one other objective [6]. While traditional MOO often involves complex evolutionary algorithms, recent adaptations for deep learning focus on gradient-based approaches suitable for network training. Applying MOO to LTR is a nascent but promising direction. For example, Mahapatra and Rajan [23] proposed a framework unifying MTL and LTR, implicitly leveraging MOO principles to balance learning across diverse class groups and tasks. Our TS-MOF explicitly formulates the second-stage fine-tuning as an MOO problem, leveraging dynamic weighting (R-PLA) and conflict-aware gradient modulation (RD-PCGrad) to achieve a balanced performance improvement across head, medium, and tail classes.

3 Methodology

To address the challenges of long-tailed image recognition, we propose a novel two-stage training framework. This framework first learns generic features through standard training and then, in the second fine-tuning stage, focuses on introducing advanced Multi-Objective Optimization (MOO) strategies to effectively leverage the complementary strengths of various long-tailed learning techniques. Compared to traditional single-stage or simpler two-stage long-tailed methods, this design allows for more flexible integration and balancing of multiple strategies, thereby achieving more balanced and comprehensive performance improvements across all parts of the long-tailed distribution. In contrast to applying MOO throughout all stages, our method simplifies the optimization process by separating feature learning and classifier adaptation. This ensures the acquisition of high-quality base features and enables the MOO in the second stage to focus more effectively and efficiently on resolving imbalance issues at the classifier level.

3.1 Stage 1: Generic Feature Pre-training

Let $\mathcal{D}_{\text{train}} = \{(x_i, y_i)\}_{i=1}^{M_{\text{train}}}$ be the long-tailed training dataset, where $x_i \in \mathcal{X}$ represents the input image, $y_i \in \mathcal{Y} = \{0, \ldots, K-1\}$ is its class label, M_{train} is the total number of training samples, and K is the total number of classes. We employ a Convolutional Neural Network (CNN) as an encoder $E(\cdot; \theta_E) : \mathcal{X} \to \mathbb{R}^{D_F}$, which maps the input image to a D_F-dimensional feature space, with parameters θ_E. This encoder is connected to a classifier head $H_{\text{S1}}(\cdot; \theta_{H_{\text{S1}}}) : \mathbb{R}^{D_F} \to \mathbb{R}^K$, with parameters $\theta_{H_{\text{S1}}}$. The objective of this stage is to learn a high-quality generic feature representation θ_E^* by minimizing the standard cross-entropy loss $\mathcal{L}_{\text{CE}}$:

$$\min_{\theta_E, \theta_{H_{\text{S1}}}} \mathbb{E}_{(x,y)\sim\mathcal{D}_{\text{train}}} \left[\mathcal{L}_{\text{CE}}\left(H_{\text{S1}}\left(E(x; \theta_E)\right), y\right)\right] \tag{1}$$

Optionally, Label Smoothing (LS) can be applied:

$$\mathcal{L}_{\text{CE\_LS}}(\mathbf{z}, y) = (1-\alpha)\mathcal{L}_{\text{CE}}(\mathbf{z}, y) + \frac{\alpha}{K}\sum_{j=0}^{K-1} \mathcal{L}_{\text{CE}}(\mathbf{z}, j) \tag{2}$$

where $\mathbf{z} \in \mathbb{R}^K$ are the logits output by the model, and α is the smoothing factor. This stage is trained for a predetermined number of epochs E_{S1}, and the encoder parameters θ_E^* that achieve the best performance on a validation set are saved.

3.2 Stage 2: Multi-Objective Long-Tailed Fine-tuning

This stage constitutes the core innovation of our method. It focuses on fine-tuning a set of classifier heads specifically designed for long-tailed distributions using advanced MOO strategies, based on the high-quality and frozen feature encoder $E(\cdot; \theta_E^*)$ obtained in the first stage. This "encoder-frozen, multi-head fine-tuning" strategy decouples the complex long-tailed problem into two phases: generic feature learning and specialized classifier adaptation, significantly reducing optimization difficulty. More importantly, it provides a flexible framework that conveniently allows various existing single-objective long-tailed learning techniques (often manifested as specific loss functions) to be transformed into independent "tasks" within our MOO framework, thereby exploring their synergistic potential.

3.2.1 Multi-Head Architecture and Task Definition

We equip the model with a multi-head output layer. Let $\mathcal{T} = \{T_1, \ldots, T_N\}$ be the set of N selected learning tasks. Each task $T_k \in \mathcal{T}$ corresponds to a specific long-tailed learning strategy and is associated with a unique loss function $\mathcal{L}_k$ and an independent classifier head $H_k(\cdot;\theta_{H_k}) : \mathbb{R}^{D_F} \to \mathbb{R}^K$. These loss functions can include standard Cross-Entropy ($\mathcal{L}_{\text{CE}}$), Balanced Softmax ($\mathcal{L}_{\text{BS}}$), Label-Distribution-Aware Margin loss ($\mathcal{L}_{\text{LDAM}}$), etc. In this fine-tuning stage, only the set of parameters for all classifier heads $\theta_H = \{\theta_{H_1}, \dots, \theta_{H_N}\}$ is optimized.

3.2.2 Multi-Objective Optimization Framework

When employing multiple tasks ($N > 1$), we face a multi-objective optimization problem, the goal of which is to simultaneously minimize the expected losses of all selected tasks:

$$\min_{\theta_H} \mathbf{L}(\theta_H) = \min_{\theta_H} (\mathbb{E}[\mathcal{L}_1(\theta_H)], \dots, \mathbb{E}[\mathcal{L}_N(\theta_H)]) \tag{3}$$

To effectively address this problem, we design and integrate the following key components:

Dynamic Task Weighting (Refined PLA) To adaptively adjust the relative importance of each task loss $\mathcal{L}_k$ in the overall optimization, we employ an improved dynamic task weighting mechanism. In each training batch of every training epoch e, for each task $T_j \in \mathcal{T}$ ($j = 1, \dots, N$), we compute its performance vector $\mathbf{a}_{j,e}^{(\text{batch})} \in \mathbb{R}^C$ on that batch's data (e.g., per-class accuracy, where C is the number of classes). These performance vectors form a list $A_e^{(\text{batch})} = \{\mathbf{a}_{1,e}^{(\text{batch})}, \dots, \mathbf{a}_{N,e}^{(\text{batch})}\}$. We designate the last performance vector in the list, $\mathbf{a}_{N,e}^{(\text{batch})}$, as the reference performance $\mathbf{a}_{\text{ref},e}^{(\text{batch})}$ for the current batch. For each performance vector $\mathbf{a}_{j,e}^{(\text{batch})}$ in the list, we compute its cosine similarity $s_{j,e}$ with the reference performance vector:

$$s_{j,e} = \frac{\mathbf{a}_{j,e}^{(\text{batch})} \cdot \mathbf{a}_{\text{ref},e}^{(\text{batch})}}{\max\left(\|\mathbf{a}_{j,e}^{(\text{batch})}\|_2 \cdot \|\mathbf{a}_{\text{ref},e}^{(\text{batch})}\|_2, \epsilon_{\text{sim}}\right)} \tag{4}$$

where ϵ_{sim} is a small positive constant ensuring numerical stability. Subsequently, the weight $\beta_{j,e}$ for task T_j is obtained by applying a cube root transformation to the similarity and performing non-negative clipping:

$$\beta_{j,e} = \max(0, \sqrt[3]{s_{j,e}}) \tag{5}$$

The cube root transformation here adjusts the sensitivity of the weights to changes in similarity. Cosine similarity, due to its insensitivity to vector magnitude, can more robustly capture similarities in performance distribution patterns among tasks in a long-tailed context, while non-negative clipping ensures the rational interpretability of weights. The weighted loss is $\mathcal{L}'_k = \beta_{k,e}\mathcal{L}_k$.

Conflict-Aware Gradient Modulation (Robust & Deterministic PCGrad) Even after task weighting, the gradients $\mathbf{g}_k = \nabla_{\theta_H}\mathcal{L}'_k \in \mathbb{R}^{D_{\text{params}}}$ (flattened vectors with respect to all trainable parameters θ_H) corresponding to different weighted losses $\mathcal{L}'_k$ may still conflict. To mitigate negative transfer, we employ a robust and deterministic PCGrad strategy. Let $G^{(0)} = \{\mathbf{g}_1, \dots, \mathbf{g}_N\}$ be the initial set of gradients, and $\mathbf{h}_k \in \{0,1\}^{D_{\text{params}}}$ be the corresponding gradient existence masks. PCGrad progressively mitigates conflicts between gradients through a series of deterministic, pairwise projection operations. For any pair of gradients $\mathbf{g}'_i$ (current state of gradient i) and $\mathbf{g}'_j$, if they conflict ($\mathbf{g}'_i \cdot \mathbf{g}'_j < 0$) and both contribute to the parameters (i.e., $\mathbf{h}_i[p] = 1 \land \mathbf{h}_j[p] = 1$ for some parameter p), then $\mathbf{g}'_i$ is modified:

$$\mathbf{g}'_i \leftarrow \mathbf{g}'_i - \frac{\mathbf{g}'_i \cdot \mathbf{g}'_j}{\|\mathbf{g}'_j\|_2^2 + \epsilon_{\text{norm}}}\mathbf{g}'_j \tag{6}$$

where $\epsilon_{\text{norm}} = 10^{-8}$ ensures numerical stability of the projection process. This procedure is applied iteratively to all gradient pairs in a fixed order, ultimately yielding a set of conflict-mitigated gradients $G_{\text{proj}} = \{\mathbf{g}''_1, \dots, \mathbf{g}''_N\}$. These projected gradients are then aggregated. For example, when using mean aggregation, the final gradient $\mathbf{g}_{\text{final}} \in \mathbb{R}^{D_{\text{params}}}$ used for parameter updates is:

$$\mathbf{g}_{\text{final}} = \frac{\sum_{k=1}^{N}(\mathbf{g}''_k \odot \mathbf{h}_k)}{\left(\sum_{k=1}^{N}\mathbf{h}_k\right) + \epsilon_{\text{div}}} \tag{7}$$

where $\odot$ denotes the Hadamard product (element-wise product), division is element-wise, and $\epsilon_{\text{div}} = 10^{-8}$ ensures numerical stability of the aggregation process. Our PCGrad implementation guarantees experimental reproducibility and enhances numerical stability.

During validation and testing phases, we implement dynamic expert opinion integration. This module learns class-specific expert weights $w_{k,c}$ based on the historical accuracy $\mathcal{A}_{\text{val}}(T_k, c)$ of each task T_k (expert) on each class c in the validation set $\mathcal{D}_{\text{val}}$:

$$w_{k,c} = \frac{\exp(\mathcal{A}_{\text{val}}(T_k, c))}{\sum_{j=1}^{N} \exp(\mathcal{A}_{\text{val}}(T_j, c)) + \epsilon_{\text{softmax}}} \tag{8}$$

where $\epsilon_{\text{softmax}}$ is a small constant to prevent division by zero. Let $\mathbf{z}_k(x) = H_k(E(x; \theta_E^*); \theta_{H_k})$ be the logits output by task T_k for input x. The final predicted probability $P_{\text{EOSS}}(y = c|x)$ is obtained by a weighted sum of the softmax probabilities from each expert head:

$$P_{\text{EOSS}}(y = c|x) = \sum_{k=1}^{N} w_{k,c} \cdot \text{softmax}(\mathbf{z}_k(x))_c \tag{9}$$

This integration method allows the model to dynamically focus on the expert that performs best on a particular class, according to its characteristics.

3.2.3 Optimization

All trainable classifier head parameters θ_H are optimized using Stochastic Gradient Descent (SGD) with momentum. The learning rate η follows a Cosine Annealing schedule, smoothly decaying from an initial value η_0 to a smaller value η_{min} over a preset number of fine-tuning epochs E_{S2} (e.g., 20 epochs in this paper).

Through this meticulously designed two-stage framework, particularly the enhanced multi-objective optimization strategy in the second stage, our method can more effectively integrate the advantages of multiple long-tailed learning techniques. The newly introduced Refined PLA mechanism, by utilizing the independent instantaneous performance of each task combined with a cube root transformation, aims to fine-tune task weights more delicately. Meanwhile, the robust and deterministic PCGrad ensures that gradient conflicts are mitigated in a stable and controllable manner. These components collectively strive to improve the model's overall performance under long-tailed distributions, especially achieving more reliable and significant improvements on challenging tail classes.

3.3 Theoretical Advantages in Robustness

Our framework, through its specific architectural choices and algorithmic components in Stage 2, exhibits notable theoretical advantages in terms of robustness. These are formalized in the following propositions.

Proposition 1 (Gradient Stability and Pareto Improvement via RD-PCGrad)**.** *Let $\mathcal{L}'_k(\theta_H)$ be the R-PLA weighted loss for task T_k and $\mathbf{g}_k = \nabla_{\theta_H}\mathcal{L}'_k(\theta_H)$ its corresponding gradient. The Robust Deterministic Projective Conflict Gradient (RD-PCGrad) mechanism, through deterministic iterative projections (Eq. 13) and numerically stabilized aggregation (Eq. 24), ensures that the final update direction $\mathbf{g}_{\mathit{final}}$ is a Pareto-improving or non-worsening direction with respect to the set of weighted objectives $\{\mathcal{L}'_k(\theta_H)\}_{k=1}^{N}$. This mitigates negative transfer between conflicting LTR strategies and enhances training stability.*

Proposition 2 (Adaptive Weighting Robustness via R-PLA)**.** *The Refined Performance Level Agreement (R-PLA) weighting scheme, defined by $\beta_{j,e} = \max(0, \sqrt[3]{s_{j,e}})$ where $s_{j,e}$ is the cosine similarity (Eq. 12), yields task weights that are robust to (i) the absolute scale of per-class performance vectors $\mathbf{a}_{j,e}^{(batch)}$, and (ii) noisy instantaneous performance estimations. The transformations ensure smoother weight dynamics, leading to a more robust adaptation of objective priorities.*

Proposition 3 (Representational Robustness via Two-Stage Decoupling)**.** *The decoupling of feature learning (Stage 1) from multi-objective classifier fine-tuning (Stage 2, with frozen θ_E^*) imbues TS-MOF with representational robustness. By fixing the feature extractor $E(\cdot; \theta_E^*)$, the MOO process is shielded from corrupting the general-purpose feature manifold, ensuring classifier balance improvements do not unduly degrade feature quality.*

Formal derivations and further theoretical justifications supporting Propositions 1-3 will be provided in the Appendix.

4 Experiment

4.1 Experimental Settings

Datasets. We conduct experiments on long-tailed image classification benchmarks: CIFAR-100-LT [3], ImageNet-LT [21], and iNaturalist 2018 [28]. CIFAR-100-LT and ImageNetLT are manually truncated long-tail versions of the original balanced dataset, while iNaturalist 2018 is a real-world dataset with a natural long tail distribution. CIFAR-100-LT has three imbalance ratio settings 10, 50, 100, and the imbalance ratio (IR) of the long tail dataset is IR=n_{max}/n_{min}, where n_{max} and n_{min} are the number of training samples in the maximum and minimum classes, respectively. For each dataset, we use the official version provided.

Evaluation Metrics. Our model performance is mainly evaluated based on the general accuracy of Top-1 (All). According to the method proposed by [1], statistical evaluations were conducted on the head, medium, and tail classes of long-tail datasets. These three classifications are as follows: many (more than 100 images), medium (20-100 images), and few (less than 20 images). All accuracy metrics are expressed as percentages.

Comparison Baselines. Multiple baseline methods were compared in the experiment, covering the main technical directions of long-tailed recognition. These loss adjustment methods include cross-entropy loss (CE) [10], category re-balancing methods such as CE-DRW [3], LDAM-DRW [3], KPS [14], Balanced Softmax (BS) [25], as well as module improvement methods such as RIDE by three experts [29], SHIKE [12] and BCL [34]. In addition, there is currently the best two-stage training strategy method, LOS [27]. We not only compare our method with these baselines, but also integrate them into our model.

Implementation. The training process is divided into two stages: feature learning and classifier fine-tuning. For each model, we use an SGD optimizer with momentum of 0.9 and weight decay of 0.005. In the feature learning stage, CIFAR-100-LT uses ResNet34 as the backbone network, with a batch size of 64 and an initial learning rate of 0.01. The learning rate was decayed by a factor of 0.1 at the 60th and 80th epochs, with a total training of 200 epochs. Freeze the backbone network parameters during the classifier fine-tuning stage, and fine tune multiple classification heads for 20 epochs using appropriate learning rates and weights. The computing resources are based on 8 NVIDIA Tesla V100 GPUs and implemented through the PyTorch framework.

Table 1: Comparison for CIFAR100-LT Benchmarks. Top-1 accuracy (%) is reported and CIFAR100-LT consists of three imbalanced ratio (IR) 10/50/100. Our model outperforms all the baselines, showing satisfactory accuracy in the few-class categories.

Method	IR=10				IR=50				IR=100			
	Head	Medium	Tail	All	Head	Medium	Tail	All	Head	Medium	Tail	All
CE [10]	63.2	40.3	–	56.5	63.9	36.2	15.2	43.8	65.6	36.2	8.2	38.1
CE - DRW [3]	62.5	48.6	–	58.2	60.6	39.0	22.9	45.0	63.4	41.2	15.7	41.4
LDAM - DRW [3]	62.7	46.1	–	57.5	63.0	41.2	25.1	47.2	62.8	42.6	21.1	43.2
BS [25]	61.5	50.6	–	58.1	60.3	41.3	34.3	47.9	59.6	42.3	23.7	42.8
RIDE (3 experts) [29]	66.4	49.4	–	61.1	65.7	47.7	31.8	52.2	65.7	48.6	25.0	47.5
BCL [34]	62.2	51.8	–	58.9	61.6	43.1	34.3	49.1	63.1	42.9	23.9	44.2
KPS [14]	61.7	58.7	–	59.5	51.6	49.5	52.4	50.5	41.9	39.5	48.7	42.2
SHIKE [12]	66.0	45.0	–	59.0	67.0	43.0	23.0	49.5	66.0	39.0	12.0	46.9
LOS [27]	71.9	62.3	–	69.0	72.4	51.4	40.2	58.0	70.3	52.3	36.6	53.9
TS-MOF	74.7	62.0	–	**70.8**	75.2	50.7	47.5	**60.2**	79.0	49.2	39.9	**56.8**

4.2 Benchmark Results

CIFAR-100-LT. Table 1 presents the overall classification accuracy results on the CIFAR-100-LT dataset, comparing the performance of single strategy and TS-MOF based strategy fusion methods. Compared to the existing SOTA model LOS [27], our method achieved performance improvements of 2.9%, 2.2%, and 1.8% respectively in the scenarios of IR=100, IR=50, and IR=10 on the CIFAR-100-LT dataset. Compared with the independent long tail learning baseline method, TS-MOF exhibits significant performance enhancement and achieves sustained and substantial improvement.

Table 2: Accuracy (%) on ImageNet-LT and iNaturalist 2018 datasets.

Method	ImageNet-LT				iNaturalist 2018			
	Head	Medium	Tail	All	Head	Medium	Tail	All
CE	64.0	33.8	5.8	41.6	73.9	63.5	55.5	61.0
CE - DRW	61.7	47.3	28.8	50.1	68.2	67.3	66.4	67.0
cRT	58.8	44.0	26.1	47.3	69.0	66.0	63.2	65.2
LDAM - DRW	60.4	46.9	30.7	49.8	–	–	–	66.1
BS	60.9	48.8	32.1	51.0	65.7	67.4	67.5	67.3
KPS	59.7	49.2	35.9	52.3	68.1	69.5	70.2	69.6
RIDE (3 experts)	64.9	50.4	34.4	53.6	69.5	71.0	70.4	70.6
BCL	65.3	53.5	36.3	55.6	69.5	70.9	71.3	70.9
LOS	63.2	50.7	42.3	54.4	69.2	70.7	71.3	70.8
TS-MOF	65.9	52.5	42.6	**56.3**	72.8	73.6	70.5	**72.3**

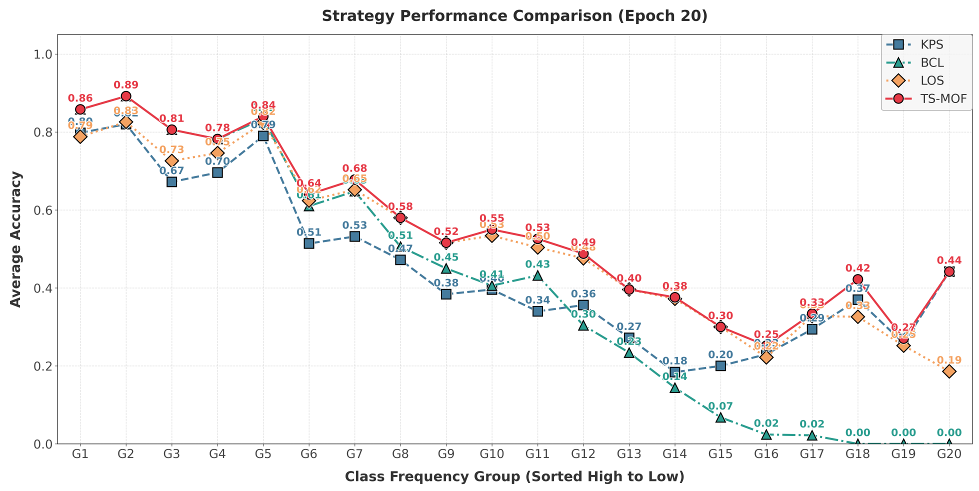

Figure 1: Performance comparison before and after policy fusion, the class frequency becomes lower from left to right.

ImageNet-LT and iNaturalist 2018. We further compared our proposed method with advanced long tail recognition methods on large-scale datasets such as ImageNet LT and iNaturalist 2018, and the results are shown in Table 2. Consistent with the conclusion in Table 1, the strategy fusion technique significantly improved the performance of the model on complex datasets.

4.3 Further Analysis

In this section, we will delve into the underlying logic of the TS-MOF mechanism and explore the following key issues. All analysis experiments were conducted based on the CIFAR-100-LT dataset (IR=100).

Figure 1 shows the performance of the TS-MOF before and after the fusion, as well as the effects of the single strategies that were merged. Clearly, after fusion, TS-MOF exhibits the advantages of fusion strategies across all classes, thus becoming more balanced.

Figures 2a, 2b, 2c, respectively, reflect the weight changes of various strategies in the head, middle, and tail. It can be seen that bcl strategy performs better in the head, the los strategy of the middle class is better than the other two strategies, and the kps strategy performs better in the tail class. This experimental result is completely consistent with Figure 2d. It is worth noting that the los strategy not only has good performance in the middle class but can also obtain relatively large weights in some tail classes. The fusion of three strategies can better leverage the performance in the head, middle, and tail to address the issue of long-tail imbalance.

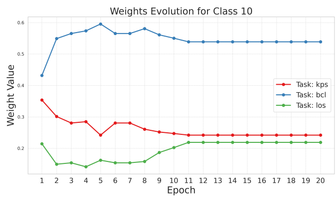

(a)

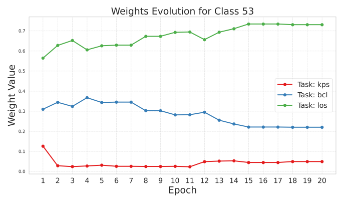

(b)

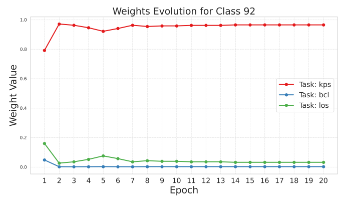

(c)

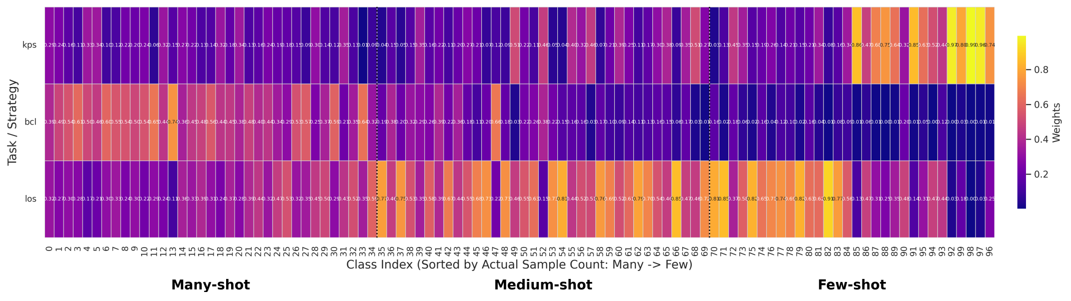

(d)

Figure 2: Further Analysis. Subfigure (a)(b)(c) show changes in strategy weights for head class, medium class and tail class. Subfigure (d) shows heatmap of strategy weights for all classes.

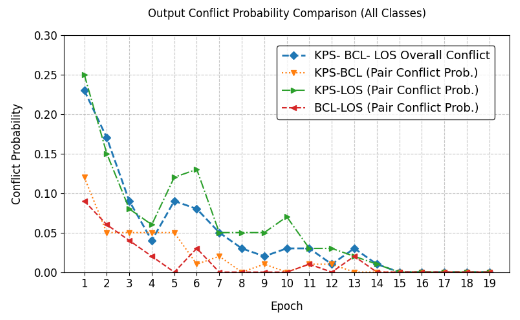

(a)

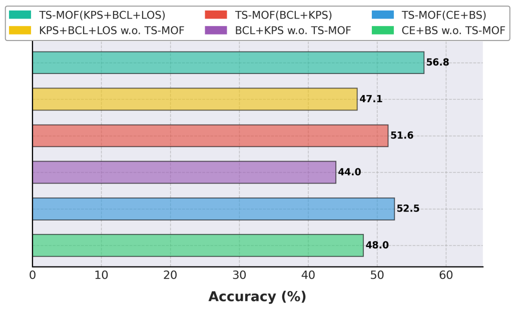

(b)

Figure 3: Further Analysis. Subfigure (a) compares the probability of output conflicts occurring when different groups of strategies are fused using TS-MOF. Subfigure (d) shows the performance improvements of our method compared to simpled weight fusion.

As shown in Figure 3a, in the initial stage of fine-tuning, the initial fusion of multiple strategies may encounter many conflicts, which can affect the fusion of strategies. However, as the epoch increases, the conflict probability of both dual strategy and triple strategy methods significantly decreases, indicating that the TS-MOF can allocate correct weights to corresponding strategies well, demonstrating the effectiveness of the TS-MOF method in conflict resolution. In Figure 3b, the performance is compared without using multi-objective optimization in policy fusion. Obviously, multi-objective optimization brings substantial benefits.

5 Conclusion

In this paper, we introduced TS-MOF, a novel Two-Stage Multi-Objective Fine-tuning framework designed to tackle the persistent challenges in Long-Tailed Recognition. By strategically decoupling robust feature pre-training from a specialized multi-objective classifier fine-tuning stage, TS-MOF significantly simplifies the integration of multiple LTR strategies. The efficacy of our approach is primarily driven by two core components in the second stage: R-PLA, which adaptively weights tasks based on their real-time performance patterns, and RD-PCGrad, which ensures stable and deterministic resolution of inter-task gradient conflicts while fostering constructive knowledge fusion.

Our extensive experiments on challenging benchmarks demonstrate that TS-MOF not only achieves state-of-the-art overall accuracy but also yields substantial improvements in tail-class performance while maintaining or even enhancing head-class accuracy, all within a highly efficient fine-tuning budget. TS-MOF provides a robust, effective, and user-friendly solution for advancing long-tailed recognition.

Acknowledgements

The authors gratefully acknowledge the support from the National Natural Science Foundation of China (NSFC) under Grant Nos. 62402472, and 12227901. This work was also supported by the Natural Science Foundation of Jiangsu Province (No. BK20240461), the Key Basic Research Foundation of Shenzhen (No. JCYJ20220818100005011), the Research Grants Council of the Hong Kong Special Administrative Region (GRF Project No. CityU 11215622), the Project of Stable Support for Youth Team in Basic Research Field, CAS (No. YSBR-005), and the Academic Leaders Cultivation Program at USTC. The AI-driven experiments, simulations and model training were performed on the robotic AI-Scientist platform of Chinese Academy of Sciences.

References

[1] Sumyeong Ahn, Jongwoo Ko, and Se-Young Yun. Cuda: Curriculum of data augmentation for long-tailed recognition. *arXiv preprint arXiv:2302.05499*, 2023.

[2] Mateusz Buda, Atsuto Maki, and Maciej A Mazurowski. A systematic study of the class imbalance problem in convolutional neural networks. *Neural networks*, 106:249–259, 2018.

[3] Kaidi Cao, Colin Wei, Adrien Gaidon, Nikos Arechiga, and Tengyu Ma. Learning imbalanced datasets with label-distribution-aware margin loss. In *Advances in neural information processing systems*, volume 32, 2019.

[4] Nitesh V Chawla, Kevin W Bowyer, Lawrence O Hall, and W Philip Kegelmeyer. Smote: synthetic minority over-sampling technique. *Journal of artificial intelligence research*, 16:321–357, 2002.

[5] Yin Cui, Menglin Jia, Tsung-Yi Lin, Yang Song, and Serge Belongie. Class-balanced loss based on effective number of samples. In *Proceedings of the IEEE/CVF conference on computer vision and pattern recognition*, pages 9268–9277, 2019.

[6] Kalyanmoy Deb. *Multi-Objective Optimization using Evolutionary Algorithms*. John Wiley & Sons, 2001.

[7] Jean-Antoine Désidéri. Multiple-gradient descent algorithm (mgda) for multiobjective optimization. *Comptes Rendus Mathematique*, 350(5-6):313–318, 2012.

[8] Jean-Antoine Désidéri. Multiple-gradient descent algorithm (mgda) for multiobjective optimization. *Comptes Rendus Mathematique*, 350(5-6):313–318, 2012.

[9] Chris Drummond, Robert C Holte, et al. C4. 5, class imbalance, and cost sensitivity: why under-sampling beats over-sampling. In *Workshop on learning from imbalanced datasets II*, volume 11, 2003.

[10] Kaiming He, Xiangyu Zhang, Shaoqing Ren, and Jian Sun. Deep residual learning for image recognition. In *Proceedings of the IEEE conference on computer vision and pattern recognition*, pages 770–778, 2016.

[11] Cong Hua, Qianqian Xu, Zhiyong Yang, Zitai Wang, Shilong Bao, and Qingming Huang. Openworldauc: Towards unified evaluation and optimization for open-world prompt tuning. *arXiv preprint arXiv:2505.05180*, 2025.

[12] Yan Jin, Mengke Li, Yang Lu, Yiu-ming Cheung, and Hanzi Wang. Long-tailed visual recognition via self-heterogeneous integration with knowledge excavation. In *Proceedings of the IEEE/CVF conference on computer vision and pattern recognition*, pages 23695–23704, 2023.

[13] Bingyi Kang, Saining Xie, Marcus Rohrbach, Zhicheng Yan, Albert Gordo, Jiashi Feng, and Yannis Kalantidis. Decoupling representation and classifier for long-tailed recognition. *arXiv preprint arXiv:1910.09217*, 2019.

[14] Mengke Li, Yiu-Ming Cheung, and Zhikai Hu. Key point sensitive loss for long-tailed visual recognition. *IEEE Transactions on Pattern Analysis and Machine Intelligence*, 45(4):4812–4825, 2022.

[15] Mengke Li, Yiu-ming Cheung, and Yang Lu. Long-tailed visual recognition via gaussian clouded logit adjustment. In *Proceedings of the IEEE/CVF conference on computer vision and pattern recognition*, pages 6929–6938, 2022.

[16] Mengke Li, Ye Liu, Yang Lu, Yiqun Zhang, Yiu-ming Cheung, and Hui Huang. Improving visual prompt tuning by gaussian neighborhood minimization for long-tailed visual recognition. *Advances in Neural Information Processing Systems*, 37:103985–104009, 2024.

[17] Mengke Li, HU Zhikai, Yang Lu, Weichao Lan, Yiu-ming Cheung, and Hui Huang. Feature fusion from head to tail for long-tailed visual recognition. In *Proceedings of the AAAI conference on artificial intelligence*, volume 38, pages 13581–13589, 2024.

[18] Sicong Li, Qianqian Xu, Zhiyong Yang, Zitai Wang, Linchao Zhang, Xiaochun Cao, and Qingming Huang. Focal-sam: Focal sharpness-aware minimization for long-tailed classification. *arXiv preprint arXiv:2505.01660*, 2025.

[19] Tsung-Yi Lin, Priya Goyal, Ross Girshick, Kaiming He, and Piotr Dollár. Focal loss for dense object detection. In *Proceedings of the IEEE international conference on computer vision*, pages 2980–2988, 2017.

[20] Jialun Liu, Yifan Sun, Chuchu Han, Zhaopeng Dou, and Wenhui Li. Deep representation learning on long-tailed data: A learnable embedding augmentation perspective. In *Proceedings of the IEEE/CVF conference on computer vision and pattern recognition*, pages 2970–2979, 2020.

[21] Ziwei Liu, Zhongqi Miao, Xiaohang Zhan, Jiayun Wang, Boqing Gong, and Stella X Yu. Large-scale long-tailed recognition in an open world. In *Proceedings of the IEEE/CVF conference on computer vision and pattern recognition*, pages 2537–2546, 2019.

[22] Yanbiao Ma, Licheng Jiao, Fang Liu, Lingling Li, Wenping Ma, Shuyuan Yang, Xu Liu, and Puhua Chen. Unveiling and mitigating generalized biases of dnns through the intrinsic dimensions of perceptual manifolds. *IEEE Transactions on Pattern Analysis and Machine Intelligence*, 2024.

[23] Debasmit Das Mahapatra, P. K. Srijith, and Balaraman Ravindran. Multi-task learning meets long-tailed recognition: A unified framework. In *Winter Conference on Applications of Computer Vision (WACV)*, pages 199–208, 2022.

[24] Aditya Krishna Menon, Sadeep Jayasumana, Ankit Singh Rawat, Himanshu Jain, Andreas Veit, and Sanjiv Kumar. Long-tail learning via logit adjustment. *arXiv preprint arXiv:2007.07314*, 2020.

[25] Jiawei Ren, Cunjun Yu, Xiao Ma, Haiyu Zhao, Shuai Yi, and et al. Balanced meta-softmax for long-tailed visual recognition. In *Advances in neural information processing systems*, volume 33, pages 4175–4186, 2020.

[26] Ozan Sener and Vladlen Koltun. Multi-task learning as multi-objective optimization. *Advances in neural information processing systems*, 31, 2018.

[27] Siyu Sun, Han Lu, Jiangtong Li, Yichen Xie, Tianjiao Li, Xiaokang Yang, Liqing Zhang, and Junchi Yan. Rethinking classifier re-training in long-tailed recognition: Label over-smooth can balance. In *The Thirteenth International Conference on Learning Representations*, 2025.

[28] Grant Van Horn, Oisin Mac Aodha, Yang Song, Yin Cui, Chen Sun, Alex Shepard, Hartwig Adam, Pietro Perona, and Serge Belongie. The inaturalist species classification and detection dataset. In *Proceedings of the IEEE conference on computer vision and pattern recognition*, pages 8769–8778, 2018.

[29] Xudong Wang, Long Lian, Zhongqi Miao, Ziwei Liu, and Stella X Yu. Long-tailed recognition by routing diverse distribution-aware experts. *arXiv preprint arXiv:2010.01809*, 2020.

[30] Zitai Wang, Qianqian Xu, Zhiyong Yang, Yuan He, Xiaochun Cao, and Qingming Huang. A unified generalization analysis of re-weighting and logit-adjustment for imbalanced learning. *Advances in Neural Information Processing Systems*, 36:48417–48430, 2023.

[31] Tianhe Yu, Saurabh Kumar, Abhishek Gupta, Sergey Levine, Karol Hausman, and Chelsea Finn. Gradient surgery for multi-task learning. In *Advances in neural information processing systems*, volume 33, pages 5824–5836, 2020.

[32] Zhe Zhao, Pengkun Wang, HaiBin Wen, Wei Xu, Song Lai, Qingfu Zhang, and Yang Wang. Two fists, one heart: multi-objective optimization based strategy fusion for long-tailed learning. In *Forty-first International Conference on Machine Learning*, 2024.

[33] Boyan Zhou, Quan Cui, Xiu-Shen Wei, and Zhao-Min Chen. Bbn: Bilateral-branch network with cumulative learning for long-tailed visual recognition. In *Proceedings of the IEEE/CVF conference on computer vision and pattern recognition*, pages 9719–9728, 2020.

[34] Jianggang Zhu, Zheng Wang, Jingjing Chen, Yi-Ping Phoebe Chen, and Yu-Gang Jiang. Balanced contrastive learning for long-tailed visual recognition. In *Proceedings of the IEEE/CVF conference on computer vision and pattern recognition*, pages 6908–6917, 2022.

[35] Eckart Zitzler and Lothar Thiele. Multiobjective optimization using evolutionary algorithms—a comparative case study. In *International conference on parallel problem solving from nature*, pages 292–301. Springer, 1998.

6 Theoretical Analysis

This appendix provides formal proofs for the three key propositions stated in Section 3.3, establishing the theoretical foundations that underpin TS-MOF's robustness and effectiveness.

6.1 Mathematical Foundations and Problem Setup

The core challenge in long-tailed recognition lies in simultaneously optimizing multiple conflicting objectives. In Stage 2 of TS-MOF, we address the multi-objective optimization problem:

$$\min_{\theta_H} \mathbf{F}(\theta_H) = (\mathbb{E}[\mathcal{L}_1(\theta_H)], \ldots, \mathbb{E}[\mathcal{L}_N(\theta_H)])^\top \tag{10}$$

where $\theta_H = \{\theta_{H_1}, \ldots, \theta_{H_N}\}$ denotes the parameters of all classifier heads, and each $\mathcal{L}_k$ represents a specific LTR strategy (e.g., Cross-Entropy, LDAM, Balanced Softmax).

The R-PLA mechanism dynamically weights these objectives based on real-time performance patterns:

$$\mathcal{L}'_k(\theta_H) = \beta_{k,e}\mathcal{L}_k(\theta_H), \quad \beta_{j,e} = \max\left(0, \sqrt[3]{s_{j,e}}\right) \tag{11}$$

where the similarity measure $s_{j,e}$ captures the alignment between task j's performance pattern and a reference:

$$s_{j,e} = \frac{\mathbf{a}_{j,e}^{(\text{batch})} \cdot \mathbf{a}_{\text{ref},e}^{(\text{batch})}}{\max\{\|\mathbf{a}_{j,e}^{(\text{batch})}\|_2 \|\mathbf{a}_{\text{ref},e}^{(\text{batch})}\|_2, \epsilon_{\text{sim}}\}} \tag{12}$$

Our theoretical analysis addresses three fundamental questions: (1) Does RD-PCGrad guarantee stable, conflict-free optimization? (2) Is R-PLA robust to noise and scaling variations? (3) Does two-stage decoupling preserve feature quality while enabling effective classifier adaptation?

6.2 Proof of Proposition 1: Gradient Stability and Pareto Improvement

Motivation: The key challenge in multi-objective LTR is that gradients from different strategies often conflict (e.g., improving tail performance may hurt head performance). RD-PCGrad must resolve these conflicts while ensuring progress toward better overall performance.

Let $\mathbf{g}_k = \nabla_{\theta_H}\mathcal{L}'_k(\theta_H) \in \mathbb{R}^D$ denote the gradient of weighted task k, where $D = |\theta_H|$ is the total number of classifier parameters.

Lemma 1 (Conflict Resolution Property)**.** *For any two conflicting gradients $\mathbf{g}_i, \mathbf{g}_j$ with $\mathbf{g}_i^\top \mathbf{g}_j < 0$, the RD-PCGrad projection:*

$$\mathbf{g}'_i = \mathbf{g}_i - \frac{\mathbf{g}_i^\top \mathbf{g}_j}{\|\mathbf{g}_j\|_2^2 + \epsilon_{norm}}\mathbf{g}_j \tag{13}$$

eliminates the conflict, ensuring $(\mathbf{g}'_i)^\top \mathbf{g}_j \geq 0$.

Proof. The key insight is that projection onto the orthogonal complement removes the conflicting component. Computing the inner product after projection:

$$(\mathbf{g}'_i)^\top \mathbf{g}_j = \left(\mathbf{g}_i - \frac{\mathbf{g}_i^\top \mathbf{g}_j}{\|\mathbf{g}_j\|_2^2 + \epsilon_{\text{norm}}}\mathbf{g}_j\right)^\top \mathbf{g}_j \tag{14}$$

$$= \mathbf{g}_i^\top \mathbf{g}_j - \frac{\mathbf{g}_i^\top \mathbf{g}_j}{\|\mathbf{g}_j\|_2^2 + \epsilon_{\text{norm}}}\|\mathbf{g}_j\|_2^2 \tag{15}$$

$$= \mathbf{g}_i^\top \mathbf{g}_j - \frac{(\mathbf{g}_i^\top \mathbf{g}_j)\|\mathbf{g}_j\|_2^2}{\|\mathbf{g}_j\|_2^2 + \epsilon_{\text{norm}}} \tag{16}$$

$$= (\mathbf{g}_i^\top \mathbf{g}_j)\left(1 - \frac{\|\mathbf{g}_j\|_2^2}{\|\mathbf{g}_j\|_2^2 + \epsilon_{\text{norm}}}\right) \tag{17}$$

$$= (\mathbf{g}_i^\top \mathbf{g}_j)\frac{\epsilon_{\text{norm}}}{\|\mathbf{g}_j\|_2^2 + \epsilon_{\text{norm}}} \tag{18}$$

Since $\mathbf{g}_i^\top \mathbf{g}_j < 0$ and $\epsilon_{\text{norm}} > 0$, we have $(\mathbf{g}'_i)^\top \mathbf{g}_j \geq 0$, resolving the conflict. □

Lemma 2 (Descent Direction Preservation). *The projection operation preserves the descent property for the objective corresponding to the projected gradient.*

Proof. We must show that $\mathbf{g}_i'$ remains a descent direction for $\mathcal{L}_i'$. The critical quantity is:

$$(\mathbf{g}_i)^\top \mathbf{g}_i' = \mathbf{g}_i^\top \left(\mathbf{g}_i - \frac{\mathbf{g}_i^\top \mathbf{g}_j}{\|\mathbf{g}_j\|_2^2 + \epsilon_{\text{norm}}} \mathbf{g}_j \right) \tag{19}$$

$$= \|\mathbf{g}_i\|_2^2 - \frac{(\mathbf{g}_i^\top \mathbf{g}_j)^2}{\|\mathbf{g}_j\|_2^2 + \epsilon_{\text{norm}}} \tag{20}$$

$$= \|\mathbf{g}_i\|_2^2 \left(1 - \frac{(\mathbf{g}_i^\top \mathbf{g}_j)^2}{\|\mathbf{g}_i\|_2^2 (\|\mathbf{g}_j\|_2^2 + \epsilon_{\text{norm}})} \right) \tag{21}$$

$$= \|\mathbf{g}_i\|_2^2 \left(1 - \frac{\cos^2(\mathbf{g}_i, \mathbf{g}_j) \|\mathbf{g}_j\|_2^2}{\|\mathbf{g}_j\|_2^2 + \epsilon_{\text{norm}}} \right) \tag{22}$$

$$> \|\mathbf{g}_i\|_2^2 \left(1 - \cos^2(\mathbf{g}_i, \mathbf{g}_j) \right) = \|\mathbf{g}_i\|_2^2 \sin^2(\mathbf{g}_i, \mathbf{g}_j) > 0 \tag{23}$$

The last inequality holds because conflicting gradients are not parallel ($\sin(\mathbf{g}_i, \mathbf{g}_j) > 0$), ensuring descent is preserved. □

Main Proof of Proposition 1: After iterative conflict resolution, RD-PCGrad produces conflict-free gradients $\{\mathbf{g}_1'', \ldots, \mathbf{g}_N''\}$ that are aggregated as:

$$\mathbf{g}_{\text{final}} = \frac{\sum_{k=1}^N (\mathbf{g}_k'' \odot \mathbf{h}_k)}{\sum_{k=1}^N \mathbf{h}_k + \epsilon_{\text{div}}} \tag{24}$$

where $\mathbf{h}_k \in \{0, 1\}^D$ are gradient existence masks and $\odot$ denotes element-wise multiplication.

Since all pairwise conflicts have been resolved, we have $(\mathbf{g}_i'')^\top \mathbf{g}_j'' \geq 0$ for all $i \neq j$. For any original gradient $\mathbf{g}_i$, the descent property with respect to the final direction is:

$$(\mathbf{g}_i)^\top \mathbf{g}_{\text{final}} = (\mathbf{g}_i)^\top \frac{\sum_{k=1}^N (\mathbf{g}_k'' \odot \mathbf{h}_k)}{\sum_{k=1}^N \mathbf{h}_k + \epsilon_{\text{div}}} \tag{25}$$

$$= \frac{\sum_{k=1}^N (\mathbf{g}_i)^\top (\mathbf{g}_k'' \odot \mathbf{h}_k)}{\sum_{k=1}^N \mathbf{h}_k + \epsilon_{\text{div}}} \tag{26}$$

$$\geq \frac{(\mathbf{g}_i)^\top (\mathbf{g}_i'' \odot \mathbf{h}_i)}{\sum_{k=1}^N \mathbf{h}_k + \epsilon_{\text{div}}} \geq 0 \tag{27}$$

where the first inequality uses the non-negativity of cross-terms after conflict resolution, and the second follows from Lemma 2. This establishes that $-\mathbf{g}_{\text{final}}$ provides a descent or non-ascent direction for all objectives, constituting a Pareto-improving or non-worsening update direction. □

6.3 Proof of Proposition 2: Adaptive Weighting Robustness

Motivation: R-PLA must maintain stable task weighting despite variations in performance measurement scales and noisy real-time estimates. The cosine similarity and cube root transformation are specifically designed to achieve this robustness.

Part (i) - Scale Invariance: Consider performance vectors scaled by factor $\lambda > 0$: $\tilde{\mathbf{a}}_{j,e} = \lambda \mathbf{a}_{j,e}$ and $\tilde{\mathbf{a}}_{\text{ref},e} = \lambda \mathbf{a}_{\text{ref},e}$. The cosine similarity becomes:

$$\tilde{s}_{j,e} = \frac{(\lambda \mathbf{a}_{j,e})^\top (\lambda \mathbf{a}_{\text{ref},e})}{\|\lambda \mathbf{a}_{j,e}\|_2 \|\lambda \mathbf{a}_{\text{ref},e}\|_2} \tag{28}$$

$$= \frac{\lambda^2 (\mathbf{a}_{j,e})^\top \mathbf{a}_{\text{ref},e}}{\lambda \|\mathbf{a}_{j,e}\|_2 \cdot \lambda \|\mathbf{a}_{\text{ref},e}\|_2} \tag{29}$$

$$= \frac{\lambda^2 (\mathbf{a}_{j,e})^\top \mathbf{a}_{\text{ref},e}}{\lambda^2 \|\mathbf{a}_{j,e}\|_2 \|\mathbf{a}_{\text{ref},e}\|_2} = s_{j,e} \tag{30}$$

Consequently, $\tilde{\beta}_{j,e} = \max(0, \sqrt[3]{\tilde{s}_{j,e}}) = \max(0, \sqrt[3]{s_{j,e}}) = \beta_{j,e}$, demonstrating perfect scale invariance.

Part (ii) - Noise Robustness: Consider noisy performance vectors $\mathbf{a}_{j,e} + \boldsymbol{\eta}_j$ where $\|\boldsymbol{\eta}_j\|_2 \leq \delta$ for small $\delta > 0$. The perturbed similarity satisfies:

$$s_{j,e}^{\text{noisy}} = \frac{(\mathbf{a}_{j,e} + \boldsymbol{\eta}_j)^\top(\mathbf{a}_{\text{ref},e} + \boldsymbol{\eta}_{\text{ref}})}{\|\mathbf{a}_{j,e} + \boldsymbol{\eta}_j\|_2\|\mathbf{a}_{\text{ref},e} + \boldsymbol{\eta}_{\text{ref}}\|_2} \tag{31}$$

$$= \frac{(\mathbf{a}_{j,e})^\top\mathbf{a}_{\text{ref},e} + (\mathbf{a}_{j,e})^\top\boldsymbol{\eta}_{\text{ref}} + \boldsymbol{\eta}_j^\top\mathbf{a}_{\text{ref},e} + \boldsymbol{\eta}_j^\top\boldsymbol{\eta}_{\text{ref}}}{\|\mathbf{a}_{j,e} + \boldsymbol{\eta}_j\|_2\|\mathbf{a}_{\text{ref},e} + \boldsymbol{\eta}_{\text{ref}}\|_2} \tag{32}$$

Using the fact that $\|\mathbf{a} + \boldsymbol{\eta}\|_2 = \|\mathbf{a}\|_2 + O(\delta)$ for small δ, and applying first-order perturbation analysis:

$$|s_{j,e}^{\text{noisy}} - s_{j,e}| \leq \frac{|(\mathbf{a}_{j,e})^\top\boldsymbol{\eta}_{\text{ref}} + \boldsymbol{\eta}_j^\top\mathbf{a}_{\text{ref},e}| + O(\delta^2)}{\|\mathbf{a}_{j,e}\|_2\|\mathbf{a}_{\text{ref},e}\|_2 + O(\delta)} \tag{33}$$

$$\leq \frac{\|\mathbf{a}_{j,e}\|_2\|\boldsymbol{\eta}_{\text{ref}}\|_2 + \|\boldsymbol{\eta}_j\|_2\|\mathbf{a}_{\text{ref},e}\|_2 + O(\delta^2)}{\|\mathbf{a}_{j,e}\|_2\|\mathbf{a}_{\text{ref},e}\|_2 + O(\delta)} \tag{34}$$

$$\leq \frac{2\delta(\|\mathbf{a}_{j,e}\|_2 + \|\mathbf{a}_{\text{ref},e}\|_2) + O(\delta^2)}{\|\mathbf{a}_{j,e}\|_2\|\mathbf{a}_{\text{ref},e}\|_2} = O(\delta) \tag{35}$$

The cube root transformation $f(x) = \max(0, \sqrt[3]{x})$ has derivative $f'(x) = \frac{1}{3}x^{-2/3}$ for $x > 0$. By the mean value theorem:

$$|\beta_{j,e}^{\text{noisy}} - \beta_{j,e}| = |f(s_{j,e}^{\text{noisy}}) - f(s_{j,e})| \tag{36}$$

$$\leq \max_{x \in [s_{j,e}^{\text{noisy}}, s_{j,e}]} |f'(x)| \cdot |s_{j,e}^{\text{noisy}} - s_{j,e}| \tag{37}$$

$$\leq \frac{1}{3}\min(s_{j,e}^{\text{noisy}}, s_{j,e})^{-2/3} \cdot O(\delta) = O(\delta) \tag{38}$$

This establishes that R-PLA weights have bounded sensitivity to noise, with the cube root transformation providing smoother weight dynamics compared to linear or quadratic functions. □

6.4 Proof of Proposition 3: Representational Robustness

Motivation: Two-stage decoupling must ensure that sophisticated MOO operations in Stage 2 do not degrade the high-quality features learned in Stage 1. This requires formal guarantees about gradient isolation and feature preservation.

Feature Quality Preservation: With encoder parameters θ_E^* frozen during Stage 2, the feature extraction mapping $E(\cdot; \theta_E^*) : \mathcal{X} \to \mathbb{R}^{D_F}$ remains constant. For any feature quality measure $Q : \mathbb{R}^{D_F} \to \mathbb{R}$ (e.g., discriminative power, cluster separability):

$$Q(E(x; \theta_E^*)) = \text{constant} \quad \forall x \in \mathcal{X}, \forall t \in \text{Stage 2 iterations} \tag{39}$$

Gradient Isolation Analysis: The Stage 2 loss functions decompose as compositions:

$$\mathcal{L}_k(\theta_H) = \mathbb{E}_{(x,y)\sim\mathcal{D}}\ell(H_k(E(x; \theta_E^*); \theta_{H_k}), y) \tag{40}$$

$$= \mathbb{E}_{(x,y)\sim\mathcal{D}}\ell(H_k(\mathbf{z}; \theta_{H_k}), y)\Big|_{\mathbf{z}=E(x;\theta_E^*)} \tag{41}$$

where $\mathbf{z} \in \mathbb{R}^{D_F}$ represents the fixed feature vectors. The gradients with respect to classifier parameters are:

$$\nabla_{\theta_{H_k}}\mathcal{L}_k(\theta_H) = \mathbb{E}_{(x,y)\sim\mathcal{D}}\nabla_{\theta_{H_k}}\ell(H_k(\mathbf{z}; \theta_{H_k}), y)\Big|_{\mathbf{z}=E(x;\theta_E^*)} \tag{42}$$

$$= \mathbb{E}_{\mathbf{z}\sim P_{\text{features}}}\nabla_{\theta_{H_k}}\ell(H_k(\mathbf{z}; \theta_{H_k}), y(\mathbf{z})) \tag{43}$$

where P_{features} is the distribution of extracted features and $y(\mathbf{z})$ is the label corresponding to feature $\mathbf{z}$.

Crucially, since θ_E^* does not appear in the optimization variables, we have:

$$\frac{\partial}{\partial \theta_E} \nabla_{\theta_{H_k}} \mathcal{L}_k(\theta_H)\Big|_{\theta_E=\theta_E^*} = \mathbf{0} \tag{44}$$

This gradient isolation ensures that MOO operations (R-PLA weighting, RD-PCGrad projections) cannot corrupt the feature representation.

Stability Under Complex MOO: The multi-objective parameter updates in Stage 2 follow:

$$\theta_H^{(t+1)} = \theta_H^{(t)} - \eta^{(t)} \mathbf{g}_{\text{final}}^{(t)} \tag{45}$$
$$\theta_E^{(t+1)} = \theta_E^{(t)} = \theta_E^* \quad \text{(architectural constraint)} \tag{46}$$

where $\mathbf{g}_{\text{final}}^{(t)} \in \mathbb{R}^{|\theta_H|}$ is computed via the sophisticated RD-PCGrad procedure but contains no components corresponding to encoder parameters.

The architectural decoupling provides an invariant: regardless of the complexity of MOO operations (dynamic weighting, gradient conflicts, iterative projections), the feature space $\{E(x; \theta_E^*) : x \in \mathcal{X}\}$ remains unchanged throughout Stage 2. This guarantees representational robustness while enabling effective classifier adaptation through MOO. □

6.5 Convergence and Complexity Analysis

Convergence Guarantee: Under standard assumptions (Lipschitz continuous gradients, bounded feasible region), TS-MOF converges to a locally Pareto-optimal solution. The key insight is that RD-PCGrad ensures:

$$\sum_{k=1}^{N} \beta_{k,e} \nabla \mathcal{L}_k(\theta_H)^\top \mathbf{g}_{\text{final}} \leq -c \|\mathbf{g}_{\text{final}}\|_2^2 \tag{47}$$

for some constant $c > 0$, providing monotonic improvement in the weighted multi-objective function.

Computational Efficiency: Stage 2 requires $O(N^2 D)$ operations per iteration, where N is the number of tasks and $D = |\theta_H|$ is the classifier parameter count. This compares favorably to end-to-end MOO requiring $O(N^2(D + D_E))$ with encoder dimension $D_E \gg D$, yielding substantial computational savings through architectural decoupling.

7 Algorithm Description

This section provides detailed algorithmic descriptions of the TS-MOF framework, with particular emphasis on the multi-objective fine-tuning process and the two core innovations: Refined Performance Level Agreement (R-PLA) and Robust Deterministic Projective Conflict Gradient (RD-PCGrad). Algorithm 1 presents the complete two-stage training procedure of TS-MOF, highlighting the strategic decoupling between feature learning and classifier adaptation.

Algorithm 1 TS-MOF: Two-Stage Multi-Objective Fine-tuning

```
Require: Long-tailed dataset $\mathcal{D}_{\text{train}}, \mathcal{D}_{\text{val}}$, LTR tasks $\mathcal{T} = \{T_1, \ldots, T_N\}$, Pre-training epochs $E_{S1}$,
    fine-tuning epochs $E_{S2}$
Ensure: Trained model with balanced performance across head, medium, and tail classes
 1: // Stage 1: Generic Feature Pre-training
 2: Initialize encoder $E(\cdot; \theta_E)$ and classifier $H_{S1}(\cdot; \theta_{H_{S1}})$
 3: for $e = 1$ to $E_{S1}$ do
 4:     for each batch $(x_i, y_i) \sim \mathcal{D}_{\text{train}}$ do
 5:         $\mathbf{z}_i \leftarrow E(x_i; \theta_E)$ {Extract features}
 6:         $\hat{y}_i \leftarrow H_{S1}(\mathbf{z}_i; \theta_{H_{S1}})$ {Classification}
 7:         $\mathcal{L}_{CE} \leftarrow$ CrossEntropy$(\hat{y}_i, y_i)$ {Standard loss}
 8:         Update $\theta_E, \theta_{H_{S1}}$ via SGD with $\mathcal{L}_{CE}$
 9:     end for
10:     Evaluate on $\mathcal{D}_{\text{val}}$ and save best $\theta_E^*$
11: end for
12: // Stage 2: Multi-Objective Classifier Fine-tuning
13: Freeze encoder parameters: $\theta_E \leftarrow \theta_E^*$ (fixed)
14: Initialize multi-head classifiers $\{H_k(\cdot; \theta_{H_k})\}_{k=1}^N$ for tasks $\mathcal{T}$
15: Initialize R-PLA weighting mechanism and RD-PCGrad optimizer
16: Call MultiObjectiveFinetuning$(E(\cdot; \theta_E^*), \{H_k\}_{k=1}^N, \mathcal{D}_{\text{train}}, E_{S2})$
17: // Inference with EOSS
18: Train EOSS weights $\{w_{k,c}\}$ based on validation performance
19: return Model with frozen $\theta_E^*$ and fine-tuned $\{\theta_{H_k}\}_{k=1}^N$
```

Algorithm 2 details the core Stage 2 process, emphasizing how R-PLA and RD-PCGrad work together to achieve effective multi-objective optimization.

Algorithm 2 Multi-Objective Fine-tuning with R-PLA and RD-PCGrad

```
Require: Frozen encoder $E(\cdot;\theta_E^*)$, classifier heads $\{H_k\}_{k=1}^N$, Training data $\mathcal{D}_{\text{train}}$, fine-tuning
    epochs $E_{S2}$, Task loss functions $\{\mathcal{L}_k\}_{k=1}^N$, number of classes $C$
Ensure: Fine-tuned classifier parameters $\{\theta_{H_k}^*\}_{k=1}^N$
 1: Initialize SGD optimizer for $\theta_H = \{\theta_{H_1}, \ldots, \theta_{H_N}\}$
 2: Initialize R-PLA weights $\{\beta_{k,e}\}_{k=1}^N$ to uniform values
 3: Initialize RD-PCGrad conflict resolution mechanism
 4: for $e = 1$ to $E_{S2}$ do
 5:     for each batch $(X, Y) \sim \mathcal{D}_{\text{train}}$ do
 6:         // Feature Extraction (Frozen)
 7:         $\mathbf{Z} \leftarrow E(X;\theta_E^*)$ {Extract fixed features}
 8:         // Multi-Head Forward Pass
 9:         logits_dict ← {}, losses_dict ← {}
10:         for $k = 1$ to $N$ do
11:             logits_dict$[k] \leftarrow H_k(\mathbf{Z};\theta_{H_k})$
12:             losses_dict$[k] \leftarrow \mathcal{L}_k($logits_dict$[k], Y)$
13:         end for
14:         // R-PLA Dynamic Weighting
15:         $\{\beta_{k,e}\}_{k=1}^N \leftarrow$ R-PLA-UPDATE(logits_dict$, Y, C$)
16:         // Apply R-PLA Weights
17:         for $k = 1$ to $N$ do
18:             $\mathcal{L}'_k \leftarrow \beta_{k,e} \cdot$ losses_dict$[k]$
19:         end for
20:         // RD-PCGrad Conflict Resolution
21:         $\mathbf{g}_{\text{final}} \leftarrow$ RD-PCGRAD$(\{\mathcal{L}'_k\}_{k=1}^N, \theta_H)$
22:         // Parameter Update
23:         $\theta_H \leftarrow \theta_H - \eta \mathbf{g}_{\text{final}}$
24:     end for
25:     Apply cosine annealing to learning rate $\eta$
26: end for
27: return $\{\theta_{H_k}^*\}_{k=1}^N$
```

Algorithm 3 presents the detailed R-PLA mechanism that adaptively weights tasks based on their real-time performance patterns and similarity to a reference performance profile.

Algorithm 3 Refined Performance Level Agreement (R-PLA) Weighting

```
Require: Logits dictionary logits_dict = $\{\text{logits}_k\}_{k=1}^N$, True labels $Y$, number of classes $C$, Numerical stability constants $\epsilon_{\text{sim}} = 10^{-8}$
Ensure: Updated task weights $\{\beta_{k,e}\}_{k=1}^N$
 1: // Compute Per-Class Performance for Each Task
 2: performance_vectors ← [ ] {Initialize empty list}
 3: for $k = 1$ to $N$ do
 4:     preds$_k$ ← $\arg\max(\text{logits}_k, \text{dim} = 1)$ {Predictions for task $k$}
 5:     $\mathbf{a}_{k,e}^{(\text{batch})}$ ← zeros($C$) {Per-class accuracy vector}
 6:     for $c = 0$ to $C - 1$ do
 7:         class_mask ← ($Y == c$) {Mask for class $c$}
 8:         total_count ← class_mask.sum()
 9:         if total_count $> 0$ then
10:             correct_count ← (preds$_k$[class_mask] $== c$).sum()
11:             $\mathbf{a}_{k,e}^{(\text{batch})}[c]$ ← correct_count/total_count
12:         else
13:             $\mathbf{a}_{k,e}^{(\text{batch})}[c]$ ← 0 {No samples for this class}
14:         end if
15:     end for
16:     performance_vectors.append($\mathbf{a}_{k,e}^{(\text{batch})}$)
17: end for
18: // Set Reference Performance (Last Task)
19: $\mathbf{a}_{\text{ref},e}^{(\text{batch})}$ ← performance_vectors[$-1$]
20: // Compute Cosine Similarity and Weights
21: for $k = 1$ to $N$ do
22:     numerator ← $\mathbf{a}_{k,e}^{(\text{batch})} \cdot \mathbf{a}_{\text{ref},e}^{(\text{batch})}$ {Dot product}
23:     denominator ← $\|\mathbf{a}_{k,e}^{(\text{batch})}\|_2 \cdot \|\mathbf{a}_{\text{ref},e}^{(\text{batch})}\|_2$
24:     $s_{k,e}$ ← $\frac{\text{numerator}}{\max(\text{denominator}, \epsilon_{\text{sim}})}$ {Cosine similarity}
25:     // Cube Root Transformation with Non-negative Clipping
26:     $\beta_{k,e}$ ← $\max(0, \sqrt[3]{s_{k,e}})$ {Robust weighting}
27: end for
28: return $\{\beta_{k,e}\}_{k=1}^N$
```

Algorithm 4 details the RD-PCGrad mechanism that resolves gradient conflicts through deterministic projections while maintaining numerical stability and reproducibility.

Algorithm 4 Robust Deterministic Projective Conflict Gradient (RD-PCGrad)

```
Require: Weighted losses $\{\mathcal{L}'_k\}_{k=1}^N$, parameters $\theta_H$
Require: Stability constants $\epsilon_{\text{norm}} = 10^{-8}$, $\epsilon_{\text{div}} = 10^{-8}$
Ensure: Conflict-resolved final gradient $\mathbf{g}_{\text{final}}$
 1: // Compute Individual Task Gradients
 2: gradients ← [ ], masks ← [ ]
 3: for $k = 1$ to $N$ do
 4:     $\mathbf{g}_k \leftarrow \nabla_{\theta_H} \mathcal{L}'_k$ {Gradient for task $k$}
 5:     $\mathbf{h}_k \leftarrow \mathbf{1}[\mathbf{g}_k \neq \mathbf{0}]$ {Gradient existence mask}
 6:     gradients.append($\mathbf{g}_k$), masks.append($\mathbf{h}_k$)
 7: end for
 8: // Deterministic Iterative Conflict Resolution
 9: projected_grads ← copy(gradients) {Deep copy for modification}
10: for $i = 1$ to $N$ do
11:     for $j = i + 1$ to $N$ do
            {Fixed pairwise order for determinism} conflict ← $(\mathbf{g}'_i)^T \mathbf{g}'_j < 0$ {Check for conflict}
            both_active ← $(\mathbf{h}_i \odot \mathbf{h}_j)$.any() {Both gradients contribute} if conflict and both_active
            then
13:         // Project gradient $i$ away from gradient $j$
16:         dot_product ← $(\mathbf{g}'_i)^T \mathbf{g}'_j$
17:         norm_squared ← $\|\mathbf{g}'_j\|_2^2 + \epsilon_{\text{norm}}$
18:         projection ← $\frac{\text{dot\_product}}{\text{norm\_squared}} \mathbf{g}'_j$
19:         $\mathbf{g}'_i \leftarrow \mathbf{g}'_i -$ projection {Remove conflicting component}
20:       end if
21:     end for
22: end for
23: // Numerically Stable Gradient Aggregation
24: weighted_grads ← [ ]
25: for $k = 1$ to $N$ do
26:     weighted_grads.append($\mathbf{g}''_k \odot \mathbf{h}_k$) {Apply existence mask}
27: end for
28: numerator ← $\sum_{k=1}^N$ weighted_grads[$k$] {Sum of masked gradients}
29: denominator ← $\sum_{k=1}^N \mathbf{h}_k + \epsilon_{\text{div}}$ {Normalization with stability}
30: $\mathbf{g}_{\text{final}} \leftarrow \frac{\text{numerator}}{\text{denominator}}$ {Element-wise division}
31: return $\mathbf{g}_{\text{final}}$
```

7.1 Key Algorithmic Innovations

Addressing the complexities of long-tailed recognition, TS-MOF incorporates several key algorithmic innovations. The **Strategic Decoupling** (Algorithm 1) tackles the challenge of simultaneously learning features and balancing classifiers by freezing the Stage 1 encoder (θ_E^*) and applying complex optimization only to the classifier heads. To navigate the conflicting goals of multiple LTR strategies, R-PLA provides **Adaptive Task Weighting** (Algorithm 3) that dynamically highlights strategies contributing most to desired performance patterns, while RD-PCGrad ensures **Deterministic Conflict Resolution** (Algorithm 4), stabilizing the multi-objective training process against negative transfer. This principled approach, coupled with **Efficient Implementation** ($O(N^2D + NC^2)$ per iteration in Stage 2), allows TS-MOF to robustly leverage complementary strengths of diverse LTR strategies, overcoming the limitations of single methods. Furthermore, our implementation simplifies the interface for integrating different strategies, practically reducing the cost of improving long-tailed learning performance using multi-objective optimization and enhancing stability.

8 Related Work: Multi-Objective Optimization in Machine Learning

Multi-Objective Optimization (MOO) is a field concerned with mathematical optimization problems involving more than one objective function to be minimized or maximized simultaneously. In many real-world scenarios and increasingly in Machine Learning (ML), multiple objectives often conflict, meaning improving one objective may degrade another. The goal of MOO is typically to find Pareto optimal solutions, where no objective can be improved without worsening at least one other.

In Machine Learning, MOO principles are naturally applied to problems involving competing goals. A prominent area is Multi-Task Learning (MTL) [**?** 35], where a single model is trained to perform multiple tasks simultaneously. Optimizing a simple weighted sum of task losses can be suboptimal, especially if tasks have conflicting gradients, leading to negative transfer [31]. This has spurred the development of gradient-based MOO methods designed to find update directions that improve all tasks or, at worst, do not worsen any, moving towards the Pareto front.

Notable gradient-based MOO methods include the Multiple-Gradient Descent Algorithm (MGDA) [8] and Projective Conflict Gradient (PCGrad) [31]. MGDA seeks to find a descent direction that minimizes the maximum directional derivative among all objectives, aiming for a common descent direction within the convex hull of the task gradients. PCGrad, on the other hand, directly addresses conflicting gradients by projecting the gradient of one task onto the normal plane of another if their dot product is negative. This iterative projection process aims to remove conflicting components, resulting in a set of modified gradients whose sum (or average) constitutes a Pareto-improving or non-worsening direction. These methods have demonstrated effectiveness in stabilizing training and improving performance in MTL scenarios.

Our approach differs significantly from existing MOO applications in ML and prior MOO-related work in LTR, driven by a specific, deeper motivation for tackling the LTR problem. While standard MOO methods like PCGrad [31] and MGDA [8] are general-purpose tools for finding Pareto solutions in arbitrary multi-objective problems (like standard MTL), **our TS-MOF framework explicitly employs MOO not as a generic optimizer for abstract tasks, but as a principled mechanism for synergistically fusing diverse, specialized LTR strategies during a targeted fine-tuning stage.** The objectives in our Stage 2 MOO are not just arbitrary task losses; they are losses derived from methods (like LDAM [3], BS [25], KPS [14], BCL [34], etc.) *specifically designed to address different aspects of the LTR imbalance*.

The deep motivation behind using MOO in TS-MOF is to move beyond the limitations of any single LTR strategy and overcome the seesaw dilemma by **finding an optimal combination that leverages the complementary strengths of multiple strategies**. R-PLA uses performance-based adaptive weighting to dynamically prioritize strategies based on their real-time contribution to the desired performance pattern, while RD-PCGrad provides a robust and deterministic way to reconcile the potentially conflicting gradient signals arising from simultaneously optimizing towards these different LTR-specific goals. We apply this advanced MOO specifically to the classifier heads after decoupling feature learning, ensuring the optimization focuses effectively on classification balance without corrupting the feature representation. Thus, our MOO is not just a mathematical technique applied; it is the core engine enabling the principled, robust, and effective fusion of heterogeneous LTR knowledge to achieve superior and balanced recognition performance.

9 More Empirical Results

This appendix provides additional empirical results and analyses to further demonstrate the effectiveness and underlying mechanisms of the TS-MOF framework.

9.1 Results on CIFAR-100-LT with Various Strategy Combinations

We also evaluated the evolutionary results of various combinations of strategies in the second stage of TS-MOF. Table 3 shows the performance across different Imbalance Ratios (IR=10, 50, 100) on the CIFAR-100-LT dataset when using TS-MOF with different sets of constituent LTR strategies. TS-MOF achieved excellent results in the combination of the KPS + BCL + LOS strategy, as highlighted in the table, demonstrating its ability to bring obvious general improvements across class groups and imbalance settings.

9.2 T-SNE Analysis

Figure 4 shows the t-SNE analysis of the feature representations from different models. We compare the representations learned by models using BCL or KPS independently, their simple weighted fusion

Table 3: Accuracy (%) on CIFAR-100-LT dataset with TS-MOF using various strategy combinations in Stage 2 fine-tuning. Results are reported for Head, Medium, Tail classes, and overall (All) accuracy across different Imbalance Ratios (IR).

Method	IR=10				IR=50				IR=100			
	Head	Medium	Tail	All	Head	Medium	Tail	All	Head	Medium	Tail	All
TS-MOF(CE+LDAM-DRW+LOS)	74.90	59.71	–	70.19	75.95	51.05	42.61	59.74	78.23	51.34	35.20	55.91
TS-MOF(CE+KPS+LOS)	74.22	62.81	–	70.68	76.22	51.63	42.06	59.99	78.46	49.14	39.57	56.53
TS-MOF(CE+BCL+LOS)	75.04	58.26	–	69.84	76.07	50.49	42.11	59.47	78.94	49.84	34.87	55.57
TS-MOF(CE+CE-DRW+LOS)	74.32	59.71	–	69.79	75.88	50.54	42.33	59.45	78.77	49.94	34.63	55.44
TS-MOF(CE+BS+LOS)	74.49	59.55	–	69.86	75.76	51.61	42.17	59.81	78.80	51.83	35.10	56.25
TS-MOF(BS+KPS+LOS)	73.99	61.42	–	70.09	75.61	53.17	42.00	**60.36**	77.49	51.54	38.27	56.64
TS-MOF(BS+BCL+LOS)	74.25	60.06	–	69.85	76.39	51.20	42.17	59.90	78.89	51.49	34.70	56.04
TS-MOF(BS+CE-DRW+LOS)	74.33	60.00	–	69.89	76.05	51.37	42.06	59.81	79.46	51.43	34.63	56.20
TS-MOF(BS+LDAM-DRW+LOS)	74.19	59.58	–	69.66	74.90	51.95	42.33	59.63	78.20	51.23	35.17	55.85
TS-MOF(KPS+BCL+LOS)	74.75	62.03	–	**70.81**	75.24	50.76	47.56	60.22	79.00	49.29	39.97	**56.89**
TS-MOF(KPS+CE-DRW+LOS)	74.52	61.68	–	70.54	75.41	51.12	45.22	60.02	78.37	50.26	38.17	56.47
TS-MOF(KPS+LDAM-DRW+LOS)	73.77	61.52	–	69.97	73.02	51.41	46.89	59.46	75.06	49.60	40.87	55.89
TS-MOF(SHIKE+BS+LOS)	74.55	59.71	–	69.95	76.22	51.39	42.11	59.90	79.03	51.77	34.77	56.21
TS-MOF(SHIKE+BCL+LOS)	74.67	59.45	–	69.95	76.15	50.73	42.28	59.63	79.17	49.66	34.73	55.51
TS-MOF(SHIKE+CE-DRW+LOS)	74.57	59.45	–	69.88	76.27	49.95	42.11	59.33	78.91	49.37	35.20	55.46
TS-MOF(SHIKE+LDAM-DRW+LOS)	74.99	59.35	–	70.14	76.15	51.15	42.22	59.79	78.40	50.74	34.73	55.62

(BCL+KPS), and our proposed fusion method TS-MOF. Compared with before fusion, the TS-MOF method shows a significantly increased separability of clusters in almost all categories in the feature space, indicating that our multi-objective fusion approach learns a more discriminative representation despite freezing the backbone in Stage 2. This suggests the classifier heads adapt in a way that better separates classes in the existing feature space.

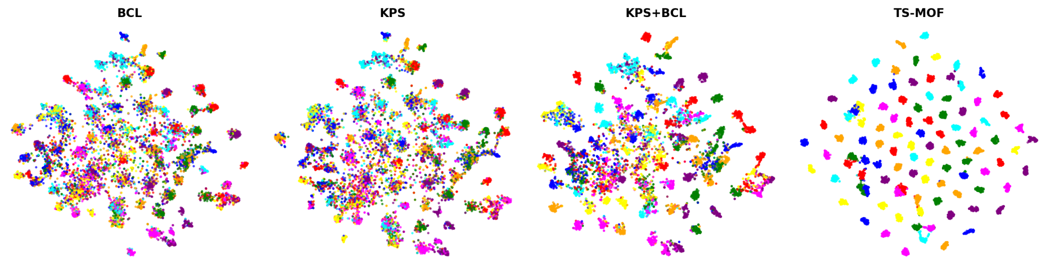

Figure 4: T-SNE comparative analysis of feature representations. We compare models trained on CIFAR-100-LT using BCL independently, KPS independently, a simple weighted fusion of BCL+KPS, and our proposed TS-MOF fusion method. Each point represents a feature vector from the test set, colored by its true class. Better separation indicates a more discriminative feature space for classification.

9.3 Confusion Matrix Analysis

Figure 5 shows a comparison of the predictive performance between individual strategies, simple fusion, and our TS-MOF method through confusion matrices. The confusion matrices are normalized by row (true label count) to show per-class accuracy patterns. From the figure, it can be seen that KPS pays more attention to some tail classes (higher diagonal values for later classes), while BCL focuses more on the head classes (higher diagonal values for earlier classes). Simple fusion may not effectively resolve conflicts and can potentially damage the performance of tail classes. Our method TS-MOF effectively combines the advantages of individual strategies and exhibits good performance across head, medium, and tail classes, as indicated by the higher and more uniform diagonal values compared to baselines and simple fusion.

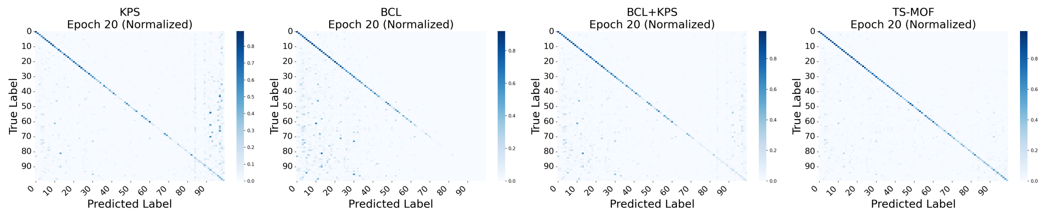

Figure 5: Comparative analysis of confusion matrices on CIFAR-100-LT (IR=100). We compare the predictive performance of models using BCL independently, KPS independently, a simple weighted fusion of BCL+KPS, and our proposed TS-MOF fusion method. Rows represent true labels, columns represent predicted labels. Diagonal elements indicate correct classifications (accuracy per class).

10 Limitations

Despite its advancements, TS-MOF has certain limitations. Its performance is inherently tied to the quality of the Stage 1 pre-trained features, as the encoder is frozen during fine-tuning. The framework also requires pre-selecting the specific set of LTR strategies to be included in the multi-objective optimization, which might require empirical tuning for optimal performance on new datasets. Furthermore, while designed for robustness, the framework still involves several hyperparameters that may need careful configuration.

11 Broader Impacts

TS-MOF aims to improve balanced recognition in long-tailed datasets, which are common in real-world applications. By enhancing tail class performance, our method can contribute to greater fairness and equity in ML systems by providing better representation for under-represented categories, potentially benefiting applications in healthcare, social sciences, and specialized domains. Making better use of rare data can also increase the utility of ML in resource-constrained settings. However, like any advanced recognition technology, there is a potential for misuse, such as in surveillance applications, emphasizing the need for responsible development and deployment.

NeurIPS Paper Checklist

1. **Claims**

   Question: Do the main claims made in the abstract and introduction accurately reflect the paper's contributions and scope?

   Answer: [Yes]

   Justification: We list our contributions in detail at the end of the Introduction.

   Guidelines:

   - The answer NA means that the abstract and introduction do not include the claims made in the paper.
   - The abstract and/or introduction should clearly state the claims made, including the contributions made in the paper and important assumptions and limitations. A No or NA answer to this question will not be perceived well by the reviewers.
   - The claims made should match theoretical and experimental results, and reflect how much the results can be expected to generalize to other settings.
   - It is fine to include aspirational goals as motivation as long as it is clear that these goals are not attained by the paper.

2. **Limitations**

   Question: Does the paper discuss the limitations of the work performed by the authors?

   Answer: [Yes]

   Justification: We discuss the limitations in Appendix.

Guidelines:

- The answer NA means that the paper has no limitation while the answer No means that the paper has limitations, but those are not discussed in the paper.
- The authors are encouraged to create a separate "Limitations" section in their paper.
- The paper should point out any strong assumptions and how robust the results are to violations of these assumptions (e.g., independence assumptions, noiseless settings, model well-specification, asymptotic approximations only holding locally). The authors should reflect on how these assumptions might be violated in practice and what the implications would be.
- The authors should reflect on the scope of the claims made, e.g., if the approach was only tested on a few datasets or with a few runs. In general, empirical results often depend on implicit assumptions, which should be articulated.
- The authors should reflect on the factors that influence the performance of the approach. For example, a facial recognition algorithm may perform poorly when image resolution is low or images are taken in low lighting. Or a speech-to-text system might not be used reliably to provide closed captions for online lectures because it fails to handle technical jargon.
- The authors should discuss the computational efficiency of the proposed algorithms and how they scale with dataset size.
- If applicable, the authors should discuss possible limitations of their approach to address problems of privacy and fairness.
- While the authors might fear that complete honesty about limitations might be used by reviewers as grounds for rejection, a worse outcome might be that reviewers discover limitations that aren't acknowledged in the paper. The authors should use their best judgment and recognize that individual actions in favor of transparency play an important role in developing norms that preserve the integrity of the community. Reviewers will be specifically instructed to not penalize honesty concerning limitations.

3. **Theory assumptions and proofs**

   Question: For each theoretical result, does the paper provide the full set of assumptions and a complete (and correct) proof?

   Answer: [Yes]

   Justification: We provide the relevant assumptions and proofs in Appendix.

   Guidelines:

   - The answer NA means that the paper does not include theoretical results.
   - All the theorems, formulas, and proofs in the paper should be numbered and cross-referenced.
   - All assumptions should be clearly stated or referenced in the statement of any theorems.
   - The proofs can either appear in the main paper or the supplemental material, but if they appear in the supplemental material, the authors are encouraged to provide a short proof sketch to provide intuition.
   - Inversely, any informal proof provided in the core of the paper should be complemented by formal proofs provided in appendix or supplemental material.
   - Theorems and Lemmas that the proof relies upon should be properly referenced.

4. **Experimental result reproducibility**

   Question: Does the paper fully disclose all the information needed to reproduce the main experimental results of the paper to the extent that it affects the main claims and/or conclusions of the paper (regardless of whether the code and data are provided or not)?

   Answer: [Yes]

   Justification: We provide code links in the abstract and implementation details in Appendix.

   Guidelines:

   - The answer NA means that the paper does not include experiments.

- If the paper includes experiments, a No answer to this question will not be perceived well by the reviewers: Making the paper reproducible is important, regardless of whether the code and data are provided or not.
- If the contribution is a dataset and/or model, the authors should describe the steps taken to make their results reproducible or verifiable.
- Depending on the contribution, reproducibility can be accomplished in various ways. For example, if the contribution is a novel architecture, describing the architecture fully might suffice, or if the contribution is a specific model and empirical evaluation, it may be necessary to either make it possible for others to replicate the model with the same dataset, or provide access to the model. In general. releasing code and data is often one good way to accomplish this, but reproducibility can also be provided via detailed instructions for how to replicate the results, access to a hosted model (e.g., in the case of a large language model), releasing of a model checkpoint, or other means that are appropriate to the research performed.
- While NeurIPS does not require releasing code, the conference does require all submissions to provide some reasonable avenue for reproducibility, which may depend on the nature of the contribution. For example
  (a) If the contribution is primarily a new algorithm, the paper should make it clear how to reproduce that algorithm.
  (b) If the contribution is primarily a new model architecture, the paper should describe the architecture clearly and fully.
  (c) If the contribution is a new model (e.g., a large language model), then there should either be a way to access this model for reproducing the results or a way to reproduce the model (e.g., with an open-source dataset or instructions for how to construct the dataset).
  (d) We recognize that reproducibility may be tricky in some cases, in which case authors are welcome to describe the particular way they provide for reproducibility. In the case of closed-source models, it may be that access to the model is limited in some way (e.g., to registered users), but it should be possible for other researchers to have some path to reproducing or verifying the results.

5. **Open access to data and code**

Question: Does the paper provide open access to the data and code, with sufficient instructions to faithfully reproduce the main experimental results, as described in supplemental material?

Answer: [Yes]

Justification: We provide the source of the dataset and code in Appendix.

Guidelines:

- The answer NA means that paper does not include experiments requiring code.
- Please see the NeurIPS code and data submission guidelines (`https://nips.cc/public/guides/CodeSubmissionPolicy`) for more details.
- While we encourage the release of code and data, we understand that this might not be possible, so "No" is an acceptable answer. Papers cannot be rejected simply for not including code, unless this is central to the contribution (e.g., for a new open-source benchmark).
- The instructions should contain the exact command and environment needed to run to reproduce the results. See the NeurIPS code and data submission guidelines (`https://nips.cc/public/guides/CodeSubmissionPolicy`) for more details.
- The authors should provide instructions on data access and preparation, including how to access the raw data, preprocessed data, intermediate data, and generated data, etc.
- The authors should provide scripts to reproduce all experimental results for the new proposed method and baselines. If only a subset of experiments are reproducible, they should state which ones are omitted from the script and why.
- At submission time, to preserve anonymity, the authors should release anonymized versions (if applicable).

- Providing as much information as possible in supplemental material (appended to the paper) is recommended, but including URLs to data and code is permitted.

6. **Experimental setting/details**

   Question: Does the paper specify all the training and test details (e.g., data splits, hyper-parameters, how they were chosen, type of optimizer, etc.) necessary to understand the results?

   Answer: [Yes]

   Justification: We describe the relevant details in Appendix.

   Guidelines:

   - The answer NA means that the paper does not include experiments.
   - The experimental setting should be presented in the core of the paper to a level of detail that is necessary to appreciate the results and make sense of them.
   - The full details can be provided either with the code, in appendix, or as supplemental material.

7. **Experiment statistical significance**

   Question: Does the paper report error bars suitably and correctly defined or other appropriate information about the statistical significance of the experiments?

   Answer: [Yes]

   Justification: We report performance metrics such as average accuracy on multiple datasets.

   Guidelines:

   - The answer NA means that the paper does not include experiments.
   - The authors should answer "Yes" if the results are accompanied by error bars, confidence intervals, or statistical significance tests, at least for the experiments that support the main claims of the paper.
   - The factors of variability that the error bars are capturing should be clearly stated (for example, train/test split, initialization, random drawing of some parameter, or overall run with given experimental conditions).
   - The method for calculating the error bars should be explained (closed form formula, call to a library function, bootstrap, etc.)
   - The assumptions made should be given (e.g., Normally distributed errors).
   - It should be clear whether the error bar is the standard deviation or the standard error of the mean.
   - It is OK to report 1-sigma error bars, but one should state it. The authors should preferably report a 2-sigma error bar than state that they have a 96% CI, if the hypothesis of Normality of errors is not verified.
   - For asymmetric distributions, the authors should be careful not to show in tables or figures symmetric error bars that would yield results that are out of range (e.g. negative error rates).
   - If error bars are reported in tables or plots, The authors should explain in the text how they were calculated and reference the corresponding figures or tables in the text.

8. **Experiments compute resources**

   Question: For each experiment, does the paper provide sufficient information on the computer resources (type of compute workers, memory, time of execution) needed to reproduce the experiments?

   Answer: [Yes]

   Justification: We mention the computational resources used for the experiments in Appendix.

   Guidelines:

   - The answer NA means that the paper does not include experiments.
   - The paper should indicate the type of compute workers CPU or GPU, internal cluster, or cloud provider, including relevant memory and storage.

- The paper should provide the amount of compute required for each of the individual experimental runs as well as estimate the total compute.
- The paper should disclose whether the full research project required more compute than the experiments reported in the paper (e.g., preliminary or failed experiments that didn't make it into the paper).

9. **Code of ethics**

   Question: Does the research conducted in the paper conform, in every respect, with the NeurIPS Code of Ethics `https://neurips.cc/public/EthicsGuidelines`?

   Answer: [Yes]

   Justification: We have read and understood the code of ethics; and have done our best to conform.

   Guidelines:

   - The answer NA means that the authors have not reviewed the NeurIPS Code of Ethics.
   - If the authors answer No, they should explain the special circumstances that require a deviation from the Code of Ethics.
   - The authors should make sure to preserve anonymity (e.g., if there is a special consideration due to laws or regulations in their jurisdiction).

10. **Broader impacts**

    Question: Does the paper discuss both potential positive societal impacts and negative societal impacts of the work performed?

    Answer: [NA]

    Justification: Our experiments are conducted on publicly available data.

    Guidelines:

    - The answer NA means that there is no societal impact of the work performed.
    - If the authors answer NA or No, they should explain why their work has no societal impact or why the paper does not address societal impact.
    - Examples of negative societal impacts include potential malicious or unintended uses (e.g., disinformation, generating fake profiles, surveillance), fairness considerations (e.g., deployment of technologies that could make decisions that unfairly impact specific groups), privacy considerations, and security considerations.
    - The conference expects that many papers will be foundational research and not tied to particular applications, let alone deployments. However, if there is a direct path to any negative applications, the authors should point it out. For example, it is legitimate to point out that an improvement in the quality of generative models could be used to generate deepfakes for disinformation. On the other hand, it is not needed to point out that a generic algorithm for optimizing neural networks could enable people to train models that generate Deepfakes faster.
    - The authors should consider possible harms that could arise when the technology is being used as intended and functioning correctly, harms that could arise when the technology is being used as intended but gives incorrect results, and harms following from (intentional or unintentional) misuse of the technology.
    - If there are negative societal impacts, the authors could also discuss possible mitigation strategies (e.g., gated release of models, providing defenses in addition to attacks, mechanisms for monitoring misuse, mechanisms to monitor how a system learns from feedback over time, improving the efficiency and accessibility of ML).

11. **Safeguards**

    Question: Does the paper describe safeguards that have been put in place for responsible release of data or models that have a high risk for misuse (e.g., pretrained language models, image generators, or scraped datasets)?

    Answer: [NA]

    Justification: Our work poses no such risks.

    Guidelines:

- The answer NA means that the paper poses no such risks.
- Released models that have a high risk for misuse or dual-use should be released with necessary safeguards to allow for controlled use of the model, for example by requiring that users adhere to usage guidelines or restrictions to access the model or implementing safety filters.
- Datasets that have been scraped from the Internet could pose safety risks. The authors should describe how they avoided releasing unsafe images.
- We recognize that providing effective safeguards is challenging, and many papers do not require this, but we encourage authors to take this into account and make a best faith effort.

12. **Licenses for existing assets**

    Question: Are the creators or original owners of assets (e.g., code, data, models), used in the paper, properly credited and are the license and terms of use explicitly mentioned and properly respected?

    Answer: [Yes]

    Justification: We are not shipping our code with any source code or binary files from any other existing libraries, so there are no concerns over getting permission or including a license. We did cite open-sourced libraries, e.g. PyTorch, in our paper.

    Guidelines:

    - The answer NA means that the paper does not use existing assets.
    - The authors should cite the original paper that produced the code package or dataset.
    - The authors should state which version of the asset is used and, if possible, include a URL.
    - The name of the license (e.g., CC-BY 4.0) should be included for each asset.
    - For scraped data from a particular source (e.g., website), the copyright and terms of service of that source should be provided.
    - If assets are released, the license, copyright information, and terms of use in the package should be provided. For popular datasets, `paperswithcode.com/datasets` has curated licenses for some datasets. Their licensing guide can help determine the license of a dataset.
    - For existing datasets that are re-packaged, both the original license and the license of the derived asset (if it has changed) should be provided.
    - If this information is not available online, the authors are encouraged to reach out to the asset's creators.

13. **New assets**

    Question: Are new assets introduced in the paper well documented and is the documentation provided alongside the assets?

    Answer: [Yes]

    Justification: We will release our code base with included readme files. We do not ship any source code or binary files from any other existing libraries.

    Guidelines:

    - The answer NA means that the paper does not release new assets.
    - Researchers should communicate the details of the dataset/code/model as part of their submissions via structured templates. This includes details about training, license, limitations, etc.
    - The paper should discuss whether and how consent was obtained from people whose asset is used.
    - At submission time, remember to anonymize your assets (if applicable). You can either create an anonymized URL or include an anonymized zip file.

14. **Crowdsourcing and research with human subjects**

    Question: For crowdsourcing experiments and research with human subjects, does the paper include the full text of instructions given to participants and screenshots, if applicable, as well as details about compensation (if any)?

Answer: [NA]

Justification: This work does not involve crowdsourcing nor research with human subjects.

Guidelines:

- The answer NA means that the paper does not involve crowdsourcing nor research with human subjects.
- Including this information in the supplemental material is fine, but if the main contribution of the paper involves human subjects, then as much detail as possible should be included in the main paper.
- According to the NeurIPS Code of Ethics, workers involved in data collection, curation, or other labor should be paid at least the minimum wage in the country of the data collector.

15. **Institutional review board (IRB) approvals or equivalent for research with human subjects**

    Question: Does the paper describe potential risks incurred by study participants, whether such risks were disclosed to the subjects, and whether Institutional Review Board (IRB) approvals (or an equivalent approval/review based on the requirements of your country or institution) were obtained?

    Answer: [NA]

    Justification: This work does not involve crowdsourcing nor research with human subjects.

    Guidelines:

    - The answer NA means that the paper does not involve crowdsourcing nor research with human subjects.
    - Depending on the country in which research is conducted, IRB approval (or equivalent) may be required for any human subjects research. If you obtained IRB approval, you should clearly state this in the paper.
    - We recognize that the procedures for this may vary significantly between institutions and locations, and we expect authors to adhere to the NeurIPS Code of Ethics and the guidelines for their institution.
    - For initial submissions, do not include any information that would break anonymity (if applicable), such as the institution conducting the review.

16. **Declaration of LLM usage**

    Question: Does the paper describe the usage of LLMs if it is an important, original, or non-standard component of the core methods in this research? Note that if the LLM is used only for writing, editing, or formatting purposes and does not impact the core methodology, scientific rigorousness, or originality of the research, declaration is not required.

    Answer: [NA]

    Justification: Our work does not involve LLMs as any important, original, or non-standard components.

    Guidelines:

    - The answer NA means that the core method development in this research does not involve LLMs as any important, original, or non-standard components.
    - Please refer to our LLM policy (`https://neurips.cc/Conferences/2025/LLM`) for what should or should not be described.